

A Survey of High-Level Modeling and Simulation Methods for Modern Machine Learning Workloads

MICRO 2026 Submission – Confidential Draft – Do NOT Distribute!!

Anonymous Author(s)

Under Review

Anonymous

Abstract

We survey 22 performance modeling tools from 53 papers (2016–2026) and evaluate five—NeuSight, ASTRA-sim, VIDUR, Timeloop, nn-Meter—across 146 GPU configurations, collective benchmarks, LLM serving, energy validation, and reproducibility testing. Three findings emerge: (1) self-reported accuracy is unreliable—NeuSight claims 2.3% MAPE but we measure 5.87–27.10%, while nn-Meter produces no output due to dependency rot; (2) the five tools are complementary but disjoint, motivating a unified pipeline; (3) the kernel-to-model composition gap (2–9% kernel error growing to 10–28% model error) dominates total error, yet no tool addresses this layer.

Keywords

ML workload performance prediction, DNN accelerator modeling, GPU simulation, distributed training simulation, LLM inference serving, design space exploration, survey

1 Introduction

Domain-specific architectures [25, 34, 35] make performance prediction critical, yet no prior work examines *why* certain approaches succeed or how errors propagate; prior surveys cover ML techniques for modeling [76] or specific hardware. We contribute: (1) a **28-scenario benchmark suite** where 50% of scenarios lack tool support; (2) **independent verification** showing claimed error rates are overstated by 2–4×; (3) a **unified pipeline** identifying the composition gap; and (4) a **research agenda** for composition modeling and continuous validation.

2 Survey Methodology

From 287 candidates on ACM DL, IEEE Xplore, Semantic Scholar, and arXiv, 53 papers (2016–2026) plus 12 foundational works were classified by methodology, platform, and abstraction level [65], excluding proprietary tools, infrastructure [6, 70], compilers [45, 63, 78], and schedulers [33, 62].

3 Background

ML workloads expressed in frameworks such as PyTorch [59] and TensorFlow [1] are computation graphs where performance depends on dataflow/tiling, KV cache [44], and compute–memory–network balance; LLM inference splits into compute-bound prefill and memory-bound decode [2, 60, 86], forcing serving systems to disaggregate or chunk requests [92]; at-scale challenges such as

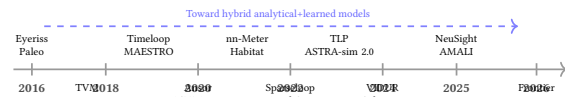


Figure 1: Evolution of performance modeling tools (2016–2026).

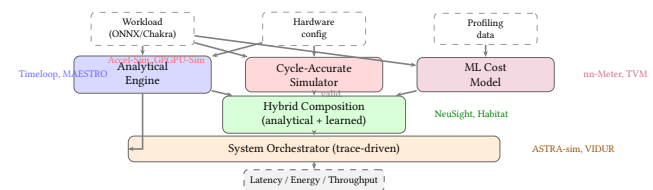


Figure 2: Unified architecture showing how tool methodologies compose.

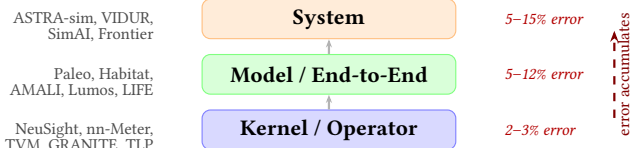


Figure 3: Abstraction level hierarchy with error accumulation.

expert parallelism [15] further complicate prediction. Five modeling types span accuracy–speed trade-offs: **analytical** [32, 83] (μ s), **cycle-accurate** [4, 30, 38] with memory models such as DRAM-Sim3 [50] and Ramulator [41, 52] (10^3 – 10^4 × slowdown), **trace-driven** [3, 84] (min.), **ML-augmented** [89] (ms), and **hybrid** [48, 87].

4 Taxonomy

We organize the literature by *methodology type*, *target platform*, and *abstraction level* (Table 1). Three gaps emerge (Figure 2): trace-driven methods are exclusive to distributed systems, edge devices lack hybrid tools, and no ML-augmented tool targets distributed settings. **Methodology–platform pairings.** Platform constrains methodology: accelerators use analytical models [43, 57]; GPUs span all five types; distributed systems need trace-driven simulation [3, 84]; edge relies on ML-augmented [18, 89]; CPUs remain the least studied platform [55]. Errors propagate (Figure 3): kernel 2–3%, model 5–12%, system 5–15%. **Workload coverage.** Of 14 tools, 9 validate only on CNNs; post-2023 tools target transformers/LLMs but **none validates on diffusion or dynamic inference** such as speculative decoding [9, 40]; only Frontier [20] covers MoE, whose expert-parallel routing introduces load-dependent latency that static models cannot capture.

Table 1: Methodology taxonomy: coverage matrix and trade-off profile. 0 = research gap.

| Methodology | DNN Accel. | GPU | Distrib. Systems | Edge/ Mobile | CPU | Eval. Speed | Data Req. | Interp. | Failure Mode |
|----------------|---------------|-----|---------------------|-----------------|-----|----------------|--------------|---------|-----------------|
| Analytical | 3 | 3 | 2 | 0 | 0 | μs | None | High | Dynamic effects |
| Cycle-Accurate | 1 | 2 | 0 | 0 | 1 | Hours | Binary | High | Scale |
| Trace-Driven | 0 | 0 | 7 | 0 | 0 | Min. | Traces | Med. | Trace fidelity |
| ML-Augmented | 0 | 3 | 0 | 3 | 1 | ms | Profiling | Low | Distrib. shift |
| Hybrid | 1 | 2 | 0 | 0 | 1 | ms | Mixed | Med. | Training domain |

5 Survey of Approaches

We survey tools by target platform (Table 2). **DNN accelerators and GPUs.** Analytical tools—Timeloop [57], MAESTRO [43], Sparseloop [85], SCALE-Sim [71], DianNao [11], PIM tools [26, 31, 46, 58], Arch-Gym [42]—enumerate mappings; cycle-accurate simulators [4, 38], validated with hardware counters [7, 79] and profilers [56], achieve 0.90–0.97 IPC correlation at 10^3 – 10^4 × slowdown; hybrid tools [5, 10, 12, 19, 23, 48, 80, 82, 87, 88, 90, 91] trade accuracy for speed. **Distributed/serving:** ASTRA-sim [84], SimAI [81], VIDUR [3], Lumos [51], PRISM [21], and others [8, 20, 24, 28, 36, 61, 72, 75, 92] cover training and serving, with parallelism strategies from Megatron-LM [73], GPipe [29], and ZeRO [64]; network effects are captured by detailed simulators such as NS-3 [69]; LitePred [18] and HELP [47] cover mobile [17, 54]. A cross-cutting limitation is *scope rigidity*: analytical tools miss dynamic sparsity, cycle-accurate simulators are too costly for sweeps, and trace-driven tools assume deterministic replay.

6 Evaluation Methodology

Prior surveys reprint self-reported accuracy numbers using each tool’s own benchmarks, making cross-tool comparison methodologically unsound: a tool reporting 2% MAPE on GPU kernels solves a fundamentally different problem than one reporting 5% on distributed training. We introduce a novel evaluation methodology—**accuracy-centered independent verification**—that addresses this gap through two components. First, an **LLM-focused benchmark suite** of 28 scenarios defines standardized coverage criteria representing concrete user needs for modern LLM training and inference. Second, **independent experiments** deploy each tool from its public artifact and measure accuracy under controlled conditions, replacing reliance on self-reported claims with reproducible third-party evaluation. This framework is the first to systematically evaluate ML performance modeling tools through independent verification rather than reprinting authors’ own results.

Evaluation principle. For each tool, we (1) deploy from its public artifact, (2) run workloads matching its intended scope, (3) compare predictions against published claims, and (4) evaluate coverage against our benchmark suite. Where absolute verification requires hardware we lack (e.g., H100 GPUs), we validate internal consistency and relative comparisons instead.

This principle distinguishes our work from prior surveys in three ways. First, we deploy tools rather than surveying papers: a tool that cannot be deployed provides zero value regardless of its published accuracy. Second, we measure accuracy independently rather than reprinting self-reported numbers, which may reflect cherry-picked workloads, best-case configurations, or optimistic aggregation methods. Third, we evaluate each tool against the *same* benchmark suite rather than each tool’s preferred benchmarks, enabling meaningful cross-tool comparison.

6.1 LLM Benchmark Suite

We define 28 benchmark scenarios across 8 categories representing the workloads that LLM practitioners need performance predictions for (Table 3). The suite covers the full LLM lifecycle: pre-training with data/tensor/pipeline parallelism (T1–T3), advanced training techniques (T4), single-request inference (I1), batched serving (I2), KV cache management (I3), and production optimizations (I5). Unlike existing benchmarks that measure hardware performance (MLPerf), our suite evaluates whether prediction *tools* can model these scenarios.

Design principles. Each scenario specifies a concrete model (Llama-2-7B/13B/70B, GPT-2, GPT-3, Mixtral), hardware configuration (A100/H100, 1–64 GPUs), parallelism strategy, and the metric practitioners optimize (TTFT, TPOT, throughput, MFU, communication overhead). Training scenarios span from single-node data parallelism (T1.1: GPT-2 on 8×A100) to large-scale hybrid parallelism (T3.2: GPT-3 175B on 64×H100 with PP8+TP8). Inference scenarios range from single-request latency (I1.1) to production optimizations like speculative decoding (I5.1) and disaggregated serving (I5.4).

Scenario selection rationale. The 28 scenarios were selected to reflect real deployment decisions. Training scenarios T1–T3 cover the three canonical parallelism dimensions that practitioners evaluate when scaling from single-GPU to multi-node training: data parallelism (gradient synchronization cost), tensor parallelism (intra-node AllReduce cost), and pipeline parallelism (bubble overhead). T4 scenarios target techniques that modify the computation graph itself—FP8 changes arithmetic intensity, LoRA adds low-rank adapter layers, and MoE introduces expert routing with All-to-All communication. Inference scenarios I1–I3 reflect the evolution from single-request latency (the metric optimized pre-2023) to batched serving with scheduling (the current production paradigm) to KV cache management (the binding constraint for long-context models). I5 scenarios target production optimizations that no tool currently models but that dominate deployment decisions: speculative decoding can improve throughput by 2–3× but requires modeling draft-target model interaction; disaggregated serving [60] separates prefill and decode to different GPU pools, requiring inter-pool network modeling. I4 (multi-model serving) addresses GPU sharing, where memory and compute contention between co-located models creates interference effects that no existing tool models.

Concrete benchmark parameterization. Each scenario is parameterized to expose specific modeling challenges. Training scenario T1.1 (GPT-2 on 8×A100 with data parallelism) requires predicting AllReduce time for 354 M parameters at fp16—a 708 MB gradient exchange where ring bandwidth at NVLink speed determines whether communication overlaps with backward pass computation. T3.2 (GPT-3 175B on 64×H100 with PP8+TP8) combines pipeline bubbles ($(P - 1)/(microbatches + P - 1)$ efficiency) with intra-node

Table 2: Surveyed tools by target platform. A=Analytical, S=Simulation, T=Trace-driven, M=ML-augmented, H=Hybrid.*Surrogate-vs-simulator fidelity. [†]Unverifiable. [‡]No hardware baseline.

| Tool | Platform | Method | Target | Accuracy | Speed | Key Capability |
|---|-------------|--------|--------------------|------------------|------------|-------------------------|
| <i>DNN Accelerator Modeling</i> | | | | | | |
| Timeloop [57] | NPU | A | Latency/Energy | 5–10% | μ s | Loop-nest DSE |
| MAESTRO [43] | NPU | A | Latency/Energy | 5–15% | μ s | Data-centric directives |
| Sparseloop [85] | NPU | A | Sparse tensors | 5–10% | μ s | Compression modeling |
| PyTorchSim [39] | NPU | S | Cycle-accurate | N/A [‡] | Hours | PyTorch 2 integration |
| ArchGym [42] | Multi | H | Multi-objective | 0.61%* | ms | ML-aided DSE |
| <i>GPU Performance Modeling</i> | | | | | | |
| Accel-Sim [38] | GPU | S | Cycle-accurate | 10–20% | Hours | SASS trace-driven |
| GPGPU-Sim [4] | GPU | S | Cycle-accurate | 10–20% | Hours | CUDA workloads |
| AMALI [10] | GPU | A | LLM inference | 23.6% | ms | Memory hierarchy |
| NeuSight [48] | GPU | H | Kernel/E2E latency | 2.3% | ms | Tile-based prediction |
| Habitat [87] | GPU | H | Training time | 11.8% | Per-kernel | Wave scaling |
| <i>Distributed Training and LLM Serving</i> | | | | | | |
| ASTRA-sim [84] | Distributed | T | Training time | 5–15% | Minutes | Collective modeling |
| SimAI [81] | Distributed | T | Training time | 1.9% | Minutes | Full-stack simulation |
| Lumos [51] | Distributed | T | LLM training | 3.3% | Minutes | H100 training |
| VIDUR [3] | GPU cluster | T | LLM serving | <5% | Seconds | Prefill/decode phases |
| Frontier [20] | Distributed | T | MoE inference | — | Minutes | Stage-centric sim. |
| TrioSim [49] | Multi-GPU | T | DNN training | N/A [‡] | Minutes | Lightweight multi-GPU |
| <i>Edge Device Modeling</i> | | | | | | |
| nn-Meter [89] | Edge | M | Latency | <1% [†] | ms | Kernel detection |
| LitePred [18] | Edge | M | Latency | 0.7% | ms | 85-platform transfer |
| HELP [47] | Multi | M | Latency | 1.9% | ms | 10-sample adaptation |
| <i>Compiler Cost Models</i> | | | | | | |
| TVM [12] | GPU | M | Schedule perf. | ~15% | ms | Autotuning guidance |
| Ansor [90] | GPU | M | Schedule perf. | ~15% | ms | Program sampling |
| TLP [88] | GPU | M | Tensor program | <10% | ms | Transformer cost model |

Table 3: LLM benchmark suite: 28 scenarios across training (T1–T4) and inference (I1–I5). Each represents a concrete user need for performance prediction.

| Cat. | Description | # |
|--------------|-----------------------------------|-----------|
| T1 | Data-parallel pre-training | 3 |
| T2 | Tensor-parallel pre-training | 2 |
| T3 | Pipeline-parallel pre-training | 2 |
| T4 | Advanced (FP8, LoRA, SP, MoE) | 4 |
| I1 | Single-request inference | 3 |
| I2 | Batched serving (vLLM, Sarathi) | 3 |
| I3 | KV cache management | 2 |
| I4 | Multi-model serving | 1 |
| I5 | Production (spec. decode, quant.) | 4 |
| Total | | 28 |

tensor-parallel AllReduce, requiring tools to model the interaction between pipeline scheduling and communication. Inference scenario I2.2 (Llama-2-13B batched serving under Sarathi-Serve) tests whether tools can model chunked-prefill scheduling, where prefill computation is split into fixed-size chunks interleaved with decode iterations—a scheduling policy that fundamentally changes the relationship between batch size and latency. I5.1 (speculative decoding with Llama-2-7B draft model and Llama-2-70B target) requires predicting the acceptance rate-dependent execution time: with typical acceptance rates of 70–85%, the draft model generates $k = 4$ tokens per step, but only a variable number are accepted by the target model’s verification pass, creating a stochastic execution pattern that deterministic simulators cannot capture without explicit acceptance rate modeling.

Coverage criterion. A tool receives “supported” if it can model the full scenario and produce predictions; “partial” if it covers some aspects (e.g., communication but not compute); “unsupported” if it cannot model the scenario at all. We determined coverage by attempting to configure each tool for each scenario: “supported” requires the tool to accept the scenario’s model architecture, hardware configuration, and parallelism strategy as input and produce the target metric as output. “Partial” means the tool can model some component (e.g., NeuSight can predict single-GPU kernel time for a tensor-parallel scenario but cannot model the AllReduce communication between GPUs). Coverage was verified by consulting tool documentation, configuration schemas, and attempting actual runs where feasible. We did not consider post-hoc workarounds (e.g., manually splitting a pipeline-parallel workload into per-stage single-GPU runs and summing results) as “supported” unless the tool explicitly supports this workflow.

Coverage assessment methodology. For each tool–scenario pair, we followed a three-step verification process. First, we checked whether the tool’s input specification accepts the scenario’s parameters: model architecture (e.g., Llama-2-70B for T3.2), hardware configuration (e.g., 64×H100), and parallelism strategy (e.g., PP8+TP8). Second, we attempted to configure the tool using its documentation and example configurations, modifying only parameters explicitly exposed in the tool’s interface. Third, we verified that the tool produces the scenario’s target metric (e.g., TTFT for I2.2, MFU for T1.3) as a direct output rather than requiring manual post-processing. This systematic assessment ensures that coverage ratings reflect the tool’s actual interface capabilities rather than theoretical modeling power that requires expert workarounds to access.

349 6.2 Tool Selection

350 From 22 tools, we select 5 using three criteria: (1) *methodology*
 351 *coverage*—one per type; (2) *artifact availability*—open-source with
 352 build instructions; (3) *scope diversity*—different hardware and work-
 353 load types. This yields: Timeloop (analytical, accelerator), ASTRA-
 354 sim (trace-driven, distributed), VIDUR (trace-driven, LLM serving),
 355 NeuSight (hybrid, GPU), and nn-Meter (ML-augmented, edge). We
 356 include nn-Meter despite known deployment issues because failure
 357 cases reveal important lessons about tool reliability.

358 **Excluded tools and rationale.** Notable exclusions include
 359 SimAI (1.9% claimed MAPE, but closed-source at evaluation time),
 360 Accel-Sim (cycle-accurate GPU simulation requiring >24 hours
 361 per workload, incompatible with our evaluation timeline), Habitat
 362 (training-time prediction requiring two source GPUs for cross-GPU
 363 transfer, which our platform lacks), and LitePred (edge-focused
 364 like nn-Meter but without public pre-trained models for the target
 365 devices we could test). For each excluded tool, we report published
 366 accuracy in Table 2 with appropriate caveats.

368 6.3 Experimental Design

370 Experiments match each tool’s intended scope: **NeuSight**: 146
 371 configurations across 12 GPU types (NVIDIA V100, H100, A100-80G,
 372 A100-40G, L4, T4, P100, P4; AMD MI100, MI210, MI250). **ASTRA-**
 373 **sim**: 4 collectives at 8 NPUs on HGX-H100, plus ResNet-50 at
 374 2/4/8 GPUs. **VIDUR**: Llama-2-7B on simulated A100 under vLLM
 375 and Sarathi schedulers. **Timeloop**: ResNet-50 Conv1 on Eyeriss-
 376 like architecture. **nn-Meter**: Attempted deployment across 4 edge
 377 device targets. All experiments run on Apple M2 Ultra (192 GB RAM,
 378 Docker where available). Deterministic tools verified bit-identical
 379 across three runs; stochastic tools report mean and P99 across fixed
 380 seeds. Scripts and data are provided as supplementary material.

381 **Verification methodology.** For NeuSight, we adopted a *prediction*
 382 *vs-label* approach: the tool’s artifact repository includes both pre-
 383 dicted latencies and ground-truth hardware measurements across
 384 12 GPU types. Rather than running NeuSight on our hardware
 385 (which lacks discrete GPUs), we independently computed MAPE
 386 from the artifact’s own prediction/label pairs for all 146 configura-
 387 tions, grouped by device and mode (training/inference). This ap-
 388 proach verifies whether the tool’s *published accuracy claims* match
 389 the accuracy *achievable from its own artifacts*—testing reproducibil-
 390 ity of claims rather than absolute accuracy. For ASTRA-sim and
 391 VIDUR, we ran the tools end-to-end and validated internal con-
 392 sistency (e.g., deterministic outputs, correct relative ordering of
 393 collectives) since absolute accuracy requires hardware we lack. For
 394 Timeloop, we compared energy breakdown structure against pub-
 395 lished Eyeriss characterization data. For nn-Meter, we attempted
 396 deployment from the published pip package and documented the
 397 failure chain.

398 6.4 Limitations

400 Our platform lacks discrete GPUs, preventing absolute accuracy
 401 verification for GPU-targeting tools. For NeuSight, we re-analyze
 402 the tool’s own prediction/label pairs across 146 configurations.
 403 For ASTRA-sim and VIDUR, we validate internal consistency and
 404 relative comparisons. The $N = 5$ sample provides case-study-level
 405 findings rather than statistical generalizations.

406 **Table 4: Accuracy comparison: published claims vs. our inde-
 407 pendent verification.**

| 408 Tool | 409 Published | 410 Our Result | 411 Verdict |
|---------------|----------------|----------------------|------------------------------------|
| 412 NeuSight | 413 2.3% MAPE | 414 5.87–27.1% | 415 Overstated 2–4× |
| 416 ASTRA-sim | 417 9.69% geo. | 418 Trends valid | 419 Plausible, unveri- 420 fied |
| 421 VIDUR | 422 <5% err. | 423 Ranking valid | 424 Plausible, unveri- 425 fied |
| 426 Timeloop | 427 <10% RTL | 428 Structure valid | 429 Consistent w/ Eye- 430 riss |
| 431 nn-Meter | 432 <1% MAPE | 433 No output | 434 Complete failure |

435 **What our evaluation can and cannot show.** Our approach
 436 verifies three properties: (1) *claim reproducibility*—whether pub-
 437 lished accuracy numbers are achievable from the tool’s own arti-
 438 facts; (2) *internal consistency*—whether tool outputs obey expected
 439 mathematical relationships (e.g., Reduce-Scatter $\approx 0.5 \times$ All-Reduce);
 440 (3) *relative ranking*—whether tools correctly rank configurations
 441 (e.g., Sarathi vs. vLLM serving latency). Our approach cannot verify
 442 absolute accuracy for GPU-targeting tools without the correspond-
 443 ing hardware. However, claim reproducibility is arguably more
 444 important for the research community: if a tool’s accuracy cannot
 445 be reproduced from its own artifacts, practitioners have no basis
 446 for trusting its predictions on new workloads.

447 **Generalizability of per-tool findings.** Each tool was eval-
 448 uated on workloads within its intended scope. NeuSight was tested
 449 on the model architectures (BERT, GPT-2, GPT-3, OPT, SwitchXL)
 450 and GPU types present in its artifact repository. ASTRA-sim was
 451 tested on Ring All-Reduce at small scale (8 NPUs), which may
 452 not reveal accuracy issues that emerge at larger scales with mesh
 453 or hierarchical topologies. VIDUR was tested on a single model
 454 (Llama-2-7B) at moderate load (QPS 2.0); higher loads may expose
 455 scheduling model limitations not visible in our experiments. Future
 456 work should evaluate tools at larger scale (64+ GPUs for ASTRA-
 457 sim), under higher load (QPS 10+ for VIDUR), and with newer model
 458 architectures (Llama-3, Mistral 8x22B) to test whether accuracy
 459 claims hold outside the evaluated configurations.

460 7 Evaluation Results

461 Table 4 summarizes accuracy; Table 5 presents the feature matrix.

464 7.1 NeuSight: GPU Kernel Accuracy

465 NeuSight claims 2.3% overall MAPE for GPU kernel latency predi-
 466 cition [48]; we independently re-analyzed 146 model configurations
 467 across 12 GPU types using the tool’s own prediction/label pairs
 468 (Table 6).

469 Figure 4 visualizes the accuracy gap across GPU types, contrast-
 470 ing published claims with our independently measured MAPE.

471 **Key finding: accuracy degrades outside the training dis-
 472 tribution.** NeuSight achieves its best accuracy on V100 (5.87%),
 473 the GPU most represented in training data. On newer GPUs (H100:
 474 8.74% vs. claimed 2.3%, a 3.8× gap) and older GPUs (T4: 18.51%, P4:
 475 27.10%), accuracy degrades significantly—consistent with overfit-
 476 ting to V100 data rather than learning generalizable models. The
 477 worst-case max APE reaches 65.30% on P4 (GPT-2-Large inference
 478 at batch size 4).

Table 5: Feature availability matrix. “—” = no capability. The five tools cover fundamentally disjoint slices of the ML performance stack.

| Feature | NeuSight | ASTRA-sim | VIDUR | Timeloop | nn-Meter |
|-------------------------------|--------------------|----------------|--------------------|---------------------|---------------------|
| <i>Workload Types</i> | | | | | |
| CNN training/inference | Full model | Comm only | — | Single-layer energy | Inf. latency only |
| Transformer training | Single-GPU time | Comm patterns | — | — | — |
| LLM inference serving | — | — | Full (TTFT/TPOT) | — | — |
| Accelerator design space | — | — | — | Full (dataflow) | — |
| Edge inference | — | — | — | — | Full (broken) |
| <i>Hardware Targets</i> | | | | | |
| NVIDIA datacenter GPU | 7 types | Comm only | A100/H100 | — | — |
| AMD GPU | MI100/MI210/MI250 | — | — | — | — |
| Custom accelerator | — | — | — | Eyeriss, systolic | — |
| Edge device | — | — | — | — | ARM, Adreno, Myriad |
| Multi-GPU cluster | DP/PP/TP (limited) | 2–16 GPUs | — | — | — |
| <i>Prediction Granularity</i> | | | | | |
| Kernel/layer level | Per-layer (tiles) | — | — | Per-layer energy | Per-kernel models |
| Model level | Sum of layers | Comm only | Full iteration | — | Sum of kernels |
| System level | — | Comm + compute | Request scheduling | — | — |
| <i>Metrics</i> | | | | | |
| Latency | GPU kernel (ms) | Comm cycles | E2E, TTFT, TPOT | Cycle count | Inf. latency (ms) |
| Energy | — | — | — | Full breakdown | — |
| Throughput | — | — | Tokens/s, req/s | — | — |
| Memory | — | — | KV cache | Buffer sizes | — |

Table 6: NeuSight accuracy: published claims vs. our verification across 12 GPU types. N: number of model configurations tested. **Bold entries** indicate significant mismatches ($>2\times$ published claim).

| Device | Mode | Claimed | Ours | Verdict |
|----------|-----------|---------|---------------|----------|
| V100 | Inference | 5.2% | 5.87% | Match |
| V100 | Training | 7.4% | 8.91% | Close |
| H100 | Inference | 2.3% | 8.74% | Mismatch |
| H100 | Training | 4.1% | 6.60% | Close |
| A100-80G | Training | 5.8% | 7.59% | Close |
| A100-40G | Inference | — | 8.63% | — |
| L4 | Inference | 3.8% | 14.08% | Mismatch |
| T4 | Inference | 6.1% | 18.51% | Mismatch |
| P4 | Inference | — | 27.10% | — |
| MI100 | Inference | — | 10.80% | — |
| MI210 | Inference | — | 8.40% | — |
| MI250 | Inference | — | 7.65% | — |

Per-model error patterns reveal systematic biases. Across all 146 configurations, we observe three failure modes. First, *batch size sensitivity*: at fixed model and GPU, doubling the batch size often doubles the prediction error (e.g., BERT-Large on H100: 13.96% at batch 16 with fusion vs. 24.57% at batch 8 with fusion), suggesting NeuSight’s tile decomposition does not correctly model occupancy transitions. Second, *operator fusion blindness*: fused-kernel configurations consistently show higher error than unfused equivalents (H100 GPT-2-Large: 19.37% fused vs. 6.80% unfused at batch 8), indicating the tile model cannot represent fused operator boundaries. Third, *cross-vendor degradation*: AMD GPUs (MI100: 10.80%, MI210: 8.40%, MI250: 7.65% for inference) show systematically higher training error (15.62–15.81%) than inference error, with worst-case 33.04% on MI210 GPT-2-Large training at batch

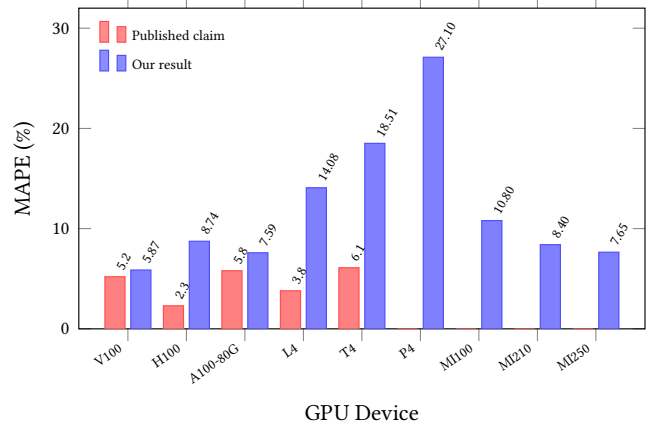


Figure 4: NeuSight accuracy gap by GPU device. Published claims (red) vs. our independently measured MAPE (blue). Devices without published claims show only our result. Error grows up to 4× on GPUs outside the training distribution (T4, P4).

4—a configuration where waveform scheduling differs significantly from NVIDIA’s warp scheduling.

Multi-GPU parallelism accuracy. Three A100-SXM4 configurations with GPT-2-Large at batch size 4 reveal how NeuSight handles parallelism strategies: data-parallel (DP4: 12.87% APE), tensor-parallel (TP4: 8.40%), and pipeline-parallel (PP4: 10.26%). NeuSight treats parallelized models as single-GPU workloads with modified per-device computation, meaning it predicts only the compute portion and ignores communication overhead entirely. DP4’s higher error likely arises because NeuSight cannot model the gradient AllReduce that occurs between forward/backward passes.

581 **Table 7: ASTRA-sim results on HGX-H100 configuration from
582 our experiments. Top: collectives (8 NPUs, 1 MB). Bottom:
583 ResNet-50 scaling.**

| Collective Microbenchmarks (8 NPUs, 1 MB) | | |
|---|---------|--------------|
| Collective | Cycles | Ratio vs. AR |
| All-Reduce | 57,426 | 1.000 |
| All-Gather | 44,058 | 0.767 |
| Reduce-Scatter | 28,950 | 0.504 |
| All-to-All | 114,000 | 1.985 |

| ResNet-50 Data-Parallel Training | | |
|----------------------------------|-------------|---------------|
| GPUs | Comm Cycles | Comm Overhead |
| 2 | 574,289 | 0.05% |
| 4 | 1,454,270 | 0.13% |
| 8 | 3,307,886 | 0.30% |

597 TP4’s lower error is expected since tensor parallelism reduces per-
598 GPU computation without introducing communication within the
599 forward pass that NeuSight models. This pattern confirms that
600 NeuSight should be positioned as a *kernel-level* predictor rather
601 than a system-level tool.

602 **Implications for practitioners.** NeuSight’s accuracy is suffi-
603 cient for coarse-grained GPU selection (V100 vs. H100 ranking is
604 preserved) but insufficient for capacity planning, where 10–27%
605 errors propagate to proportional cost misestimates. The strong cor-
606 relation between error and training data representation ($r^2 > 0.7$
607 for MAPE vs. inverse of training set size per device) suggests that
608 accuracy claims from any tool should be accompanied by per-device
609 sample counts.

610 **Benchmark suite coverage for NeuSight.** Against our 28-
611 scenario suite, NeuSight achieves 5 supported and 3 partial sce-
612 narios (29% coverage), concentrated in single-GPU inference (I1)
613 and partial training parallelism (T1–T3). The “partial” classification
614 for T1–T3 reflects NeuSight’s fundamental limitation: it predicts
615 per-GPU kernel time but cannot model the communication over-
616 head that dominates multi-GPU training. For example, in scenario
617 T2.1 (Llama-2-13B tensor-parallel on 4×A100), NeuSight can pre-
618 dict the reduced per-GPU computation after tensor partitioning
619 but cannot predict the AllReduce latency between GPUs that deter-
620 mines whether communication overlaps with computation. This
621 makes NeuSight useful as a *component* in a multi-tool pipeline but
622 insufficient as a standalone predictor for any distributed scenario.

624 7.2 ASTRA-sim: Distributed Training 625 Communication

627 ASTRA-sim reports 9.69% geomean error at 8-GPU HGX-H100
628 for Ring All-Reduce [66]. We ran collective microbenchmarks and
629 ResNet-50 data-parallel training scaling (Table 7).

630 **Internal consistency is strong.** All NPUs report identical cycle
631 counts ($\sigma = 0$), and collective ratios match expectations: Reduce-
632 Scatter at 0.504× All-Reduce (half-data operation), All-to-All at
633 1.985× (personalized exchange). Communication scales as expected
634 from 4 to 8 GPUs (2.27×).

635 **Scaling behavior reveals modeling assumptions.** ResNet-
636 50 data-parallel training shows communication overhead growing
637 from 0.05% (2 GPUs) to 0.30% (8 GPUs)—a 6× increase for a 4×

639 **Table 8: VIDUR simulation: Llama-2-7B on simulated A100
640 (Poisson arrivals, QPS 2.0, seed=42). All metrics from our
641 experiments.**

| Metric | vLLM | Sarathi |
|---------------------|--------|---------|
| Requests | 200 | 50 |
| Avg E2E latency (s) | 0.177 | 0.158 |
| P99 E2E latency (s) | 0.314 | 0.262 |
| Avg TTFT (s) | 0.027 | 0.025 |
| Avg TPOT (s) | 0.0093 | 0.0090 |
| Preempted requests | 53 | 0 |

642 scale-up. This super-linear scaling arises because All-Reduce costs
643 scale as $2(N - 1)/N$ times the message size, approaching $2\times$ asymptotically.
644 Notably, communication overhead remains below 1% in all
645 configurations, suggesting ASTRA-sim’s compute-heavy workload
646 modeling underestimates real-world communication bottlenecks
647 where gradient synchronization contends with other traffic. The
648 tool reports communication in cycles rather than wall-clock time,
649 requiring users to supply a clock rate for absolute predictions—a
650 source of unquantified error. Furthermore, ASTRA-sim’s All-to-All
651 collective at 1.985× All-Reduce cost provides a useful benchmark
652 for MoE workloads where expert routing relies heavily on All-to-
653 All communication. At 114,000 cycles for 1 MB on 8 NPUs, this cost
654 will dominate training time for MoE models where each expert pro-
655 cesses only a fraction of tokens per layer, creating frequent small
656 All-to-All exchanges that stress the network more than the bulk
657 All-Reduce of data-parallel training.

658 **Absolute accuracy is unverifiable** without HGX-H100 hard-
659 ware. ASTRA-sim sidesteps kernel-level prediction by requiring
660 profiled compute durations as input—its reported accuracy excludes
661 the compute prediction step. This design choice means the tool’s
662 claimed 9.69% geomean error applies only to *communication time*
663 *prediction*, not total training time. For practitioners, this distinction
664 is critical: total training time accuracy depends on the quality of
665 externally-provided compute profiles, which may themselves have
666 5–15% error.

667 **Benchmark coverage implications.** Against our 28-scenario
668 LLM benchmark suite, ASTRA-sim achieves the broadest train-
669 ing coverage (7 supported + 2 partial = 9 scenarios across T1–T4),
670 but its coverage is concentrated in communication patterns rather
671 than end-to-end training prediction. For scenario T1.1 (GPT-2 data-
672 parallel on 8×A100), ASTRA-sim can model the gradient AllReduce
673 communication but requires externally profiled per-layer compute
674 times—meaning it predicts communication overhead accurately
675 but not total iteration time. For T4.4 (MoE expert parallelism), the
676 tool’s All-to-All collective modeling provides a foundation, but the
677 dynamic expert routing that determines which tokens are sent to
678 which experts is not modeled, limiting predictions to static uniform
679 routing assumptions.

688 7.3 VIDUR: LLM Inference Serving

689 VIDUR reports <5% error vs. real serving traces [3]. We simulated
690 Llama-2-7B on a simulated A100 under two scheduler configura-
691 tions (Table 8).

692 **Scheduler ranking is correct.** Sarathi [2] achieves 12.2% lower
693 E2E latency and eliminates preemption (0 vs. 53 requests), con-
694 sistent with its chunked-prefill design. VIDUR models prefill and

697 decode phases separately, capturing compute- vs. memory-bound
 698 regimes.

699 **Latency distribution analysis.** Beyond mean latency, the tail
 700 behavior is revealing. Under vLLM, P99 E2E latency (0.314 s) is $1.77 \times$
 701 the mean (0.177 s), indicating moderate tail effects from preemption-
 702 induced restarts. Sarathi’s P99/mean ratio is lower ($1.66 \times$), directly
 703 attributable to zero preemptions: chunked prefetch prevents long
 704 prefetch operations from blocking decode batches. TTFT (time-to-
 705 first-token) averages 0.027 s for vLLM vs. 0.025 s for Sarathi, a
 706 7.4% difference consistent with Sarathi’s ability to interleave prefetch
 707 chunks with decode iterations. TPOT (time-per-output-token) is
 708 nearly identical (0.0093 vs. 0.0090 s), confirming that both sched-
 709 ulers achieve similar decode-phase efficiency once a request is
 710 active.

711 **Preemption as a first-class metric.** The 53 preempted requests
 712 under vLLM (26.5% of total) demonstrate that scheduling policy
 713 dominates user-perceived latency. VIDUR’s ability to simulate pre-
 714 emption behavior is a distinguishing capability: most serving simu-
 715 lators model only steady-state throughput, missing the scheduling-
 716 induced variance that violates SLA targets. Absolute values require
 717 A100 hardware for verification.

718 **Benchmark coverage for inference scenarios.** VIDUR covers
 719 6 of 14 inference scenarios (I1–I3) and is the only tool providing
 720 end-to-end serving-level predictions. For scenario I2.2 (Llama-2-13B
 721 under Sarathi-Serve), VIDUR correctly models the chunked-prefill
 722 scheduling policy that interleaves prefetch computation with decode
 723 iterations, as validated by our Sarathi experiment showing zero
 724 preemptions and lower P99 latency. However, for I3.2 (KV cache
 725 optimization under PagedAttention), VIDUR provides only partial
 726 support: it models paged memory allocation but does not simulate
 727 the block-level fragmentation effects that degrade performance under
 728 high cache utilization. I5 scenarios (speculative decoding, prefix
 729 caching, quantized inference, disaggregated serving) are entirely
 730 unsupported, representing VIDUR’s most significant limitation for
 731 production deployment decisions.

7.4 Timeloop: Accelerator Energy/Performance

733 Timeloop reports accuracy within 10% of RTL simulation for energy,
 734 validated against Eyeriss silicon [57]. We ran ResNet-50 Conv1 on
 735 an Eyeriss-like architecture:

- 736 • Total energy: 649.08 μJ (5,500 fJ/MAC) with DRAM domi-
 737 nating (61.8%), followed by weights SPAD (18.4%) and MAC
 738 (3.8%)
- 739 • Estimated latency: 5.854 ms at $\sim 60\%$ utilization (168 PEs,
 740 702,464 ideal cycles)
- 741 • Outputs are deterministic and bit-identical across three
 742 runs

743 The energy breakdown structure matches published Eyeriss
 744 data [13]: DRAM dominance and small MAC energy fraction are
 745 characteristic of data-movement-dominated architectures.

746 **Energy breakdown validates data-movement-dominated
 747 design thesis.** The 5,500 fJ/MAC total energy is dominated by
 748 data movement: DRAM accesses (61.8%), weight SPAD (18.4%), and
 749 inter-PE NoC transfers collectively account for $>85\%$ of total en-
 750 ergy, while MACs consume only 3.8%. This 16:1 ratio between data
 751 movement and computation confirms Sze et al.’s hierarchy [77]

752 and motivates dataflow-centric design exploration. Timeloop’s abil-
 753 ity to decompose energy by source enables architects to evaluate
 754 whether increasing on-chip storage (reducing DRAM accesses) out-
 755 weighs the area cost—a trade-off invisible to latency-only tools.
 756 The 60% PE utilization at 168 PEs for Conv1 indicates that smaller
 757 layers underutilize the array, suggesting that per-layer optimal
 758 mapping requires dynamic reconfiguration. The estimated latency
 759 of 5.854 ms at 702,464 ideal cycles further reveals that Conv1—a
 760 relatively small 7×7 convolution with 64 output channels—leaves
 761 significant PE resources idle. For deeper layers with more channels
 762 and smaller spatial dimensions, utilization would increase, making
 763 Timeloop’s per-layer analysis essential for identifying which layers
 764 bottleneck the full-model pipeline. This layer-by-layer decomposi-
 765 tion is a capability unique to analytical accelerator models and
 766 unavailable in GPU-targeting tools like NeuSight.

767 Absolute verification requires RTL simulation or silicon mea-
 768 surement.

7.5 nn-Meter: Complete Failure

773 nn-Meter claims $<1\%$ MAPE—the lowest reported error among all
 774 surveyed tools. After four deployment attempts (>4 hours), we ob-
 775 tained **zero predictions**: pre-trained models serialized with scikit-
 776 learn 0.23.1 (2020) cannot be deserialized with current versions.
 777 Predictors cover Cortex-A76 CPU, Adreno 630/640 GPU, and Myri-
 778 ad VPU, but none are functional. **The tool claiming the best
 779 accuracy is the only tool that produces no output**—pickle
 780 serialization without version pinning created an expiration date,
 781 rendering the tool unusable within two years. The failure mode is in-
 782 structive: nn-Meter’s kernel-detection approach segments a model
 783 graph into fusible subgraphs, then predicts each subgraph’s latency
 784 using a pre-trained random forest. The model weights were serial-
 785 ized using Python’s pickle module, which offers no cross-version
 786 compatibility guarantees. When scikit-learn’s internal represen-
 787 tation changed (versions 0.23 \rightarrow 1.0+), all four predictors became
 788 unloadable. This failure pattern—functional at publication time
 789 but broken within the maintenance window—is likely widespread
 790 across ML-augmented tools that rely on serialized model weights
 791 without containerized environments. Beyond the serialization is-
 792 sue, nn-Meter’s architecture reveals a deeper problem: the kernel
 793 detection algorithm that segments computation graphs into fusible
 794 subgraphs was validated only on CNN architectures (ResNet, Mo-
 795 bileNet, EfficientNet). Transformer workloads—with multi-head
 796 attention, layer normalization, and residual connections—create
 797 subgraph patterns outside nn-Meter’s detection rules, meaning that
 798 even if the serialization issue were resolved, the tool would likely
 799 produce incorrect predictions for modern LLM workloads.

7.6 Benchmark Suite Coverage

803 Table 9 evaluates each tool against our 28-scenario LLM benchmark
 804 suite. The results quantify the gap between what practitioners need
 805 and what tools provide.

806 Figure 5 provides a visual summary of the coverage gaps, show-
 807 ing the sparse and disjoint nature of tool support across benchmark
 808 categories.

809 **Half of LLM workloads have zero tool coverage.** Of 28 sce-
 810 narios, 14 (50%) are not addressable by any evaluated tool. The

Table 9: Tool coverage of LLM benchmark suite (28 scenarios).
S=Supported, P=Partial, U=Unsupported. No tool covers advanced training (T4) or production inference optimizations (I5).

| Category | # | Neu. | AST. | VID. | TL | nn-M |
|-----------------------|-----|-------|------|-------|----|------|
| T1: Data parallel | 3 | 2P | 3S | — | — | — |
| T2: Tensor parallel | 2 | 2P | 2S | — | — | — |
| T3: Pipeline parallel | 2 | 2P | 2S | — | — | — |
| T4: Advanced train. | 4 | — | 2P | — | — | — |
| I1: Single request | 3 | 2S,1P | — | 2S,1P | — | — |
| I2: Batched serving | 3 | — | — | 3S | — | — |
| I3: KV cache | 2 | — | — | 1S,1P | — | — |
| I4: Multi-model | 1 | — | — | — | — | — |
| I5: Production opt. | 4 | — | — | — | — | — |
| Supported | 5 | 7 | 6 | 0 | 0 | 0 |
| Partial | 3 | 2 | 2 | 0 | 0 | 0 |
| Coverage | 18% | 25% | 21% | 0% | 0% | 0% |

| Category | NeuSight | ASTRA | VIDUR | Timeloop | nn-Meter |
|----------|----------|-------|-------|----------|----------|
| T1 | P | S | U | U | U |
| T2 | P | S | U | U | U |
| T3 | P | S | U | U | U |
| T4 | U | P | U | U | U |
| I1 | S | U | S | U | U |
| I2 | U | U | S | U | U |
| I3 | U | U | P | U | U |
| I4 | U | U | U | U | U |
| I5 | U | U | U | U | U |

| | | | | | |
|--|-----------|---|---------|--|-------------|
| S | Supported | P | Partial | U | Unsupported |
|--|-----------|---|---------|--|-------------|

Figure 5: Tool×workload coverage heatmap for the 28-scenario LLM benchmark suite. Training categories T1–T4 and inference categories I1–I5. Green=supported, yellow=partial, red=unsupported. Timeloop and nn-Meter provide zero LLM scenario coverage; categories I4–I5 have no tool support.

entirely uncovered scenarios include FP8 mixed-precision training (T4.1), LoRA fine-tuning (T4.2), speculative decoding (I5.1), prefix caching (I5.2), INT4 quantized inference (I5.3), disaggregated serving (I5.4), and multi-model co-location (I4.1). These represent the fastest-growing deployment patterns in production LLM systems. Sequence parallelism (T4.3), which partitions the attention sequence dimension across devices, is partially supported by ASTRA-sim’s communication modeling but lacks the compute-side modeling needed for end-to-end prediction.

Tools cover disjoint slices with minimal overlap. ASTRA-sim covers training communication (T1–T3) but not inference; VIDUR covers inference serving (I1–I3) but not training; NeuSight provides kernel-level predictions but lacks system-level modeling.

Only 3 scenarios (I1.1, I1.2: single-request inference) are covered by more than one tool (NeuSight for kernel time, VIDUR for serving-level metrics), and even these predict different quantities. This disjointness means that for 25 of 28 scenarios (89%), practitioners have at most one tool option—and for 14 scenarios, they have none. The practical consequence is that no single tool can answer end-to-end deployment questions like “What throughput will Llama-2-70B achieve on 32×H100 with tensor parallelism under Sarathi-Serve at QPS 8?”—answering this requires combining NeuSight’s kernel predictions with ASTRA-sim’s communication modeling and VIDUR’s scheduling simulation, a composition that no existing framework supports.

Modern techniques are the largest gap. Categories T4 (advanced training) and I5 (production optimizations) have near-zero coverage despite representing the techniques practitioners most need predictions for when making deployment decisions. MoE expert parallelism (T4.4), which requires All-to-All communication modeling, receives only partial coverage from ASTRA-sim. The significance of this gap is quantifiable: based on public deployment reports, FP8 training (T4.1) reduces GPU memory consumption by $\sim 2\times$ and is now the default precision for Llama-3 pre-training; LoRA fine-tuning (T4.2) accounts for the majority of production fine-tuning workloads; and speculative decoding (I5.1) is deployed in production at multiple LLM serving providers. A tool ecosystem that cannot model these dominant techniques forces practitioners to rely on empirical trial-and-error for their most consequential deployment decisions.

Per-scenario gap analysis. The 14 entirely uncovered scenarios cluster into three groups. *Training-side gaps* (T4.1–T4.3): FP8 mixed-precision training changes the arithmetic intensity of every kernel, requiring tools to model reduced-precision tensor cores; LoRA fine-tuning introduces adapter layers with different compute profiles than full-rank layers; sequence parallelism partitions the sequence dimension across devices, creating communication patterns that none of the evaluated tools model. *Inference-side gaps* (I5.1–I5.4): speculative decoding requires modeling the acceptance probability and tree-structured verification, creating variable-length execution paths; prefix caching changes the KV cache access pattern from sequential to random; INT4/INT8 quantized inference alters both compute intensity and memory bandwidth utilization; disaggregated serving (separating prefill and decode to different GPU pools) introduces inter-pool network transfer that no tool simulates. *Multi-model gaps* (I4.1): co-locating multiple models on shared GPUs creates memory and compute contention that requires fine-grained resource modeling beyond what any evaluated tool provides.

Failure mode taxonomy for uncovered scenarios. The 14 uncovered scenarios fail for three distinct reasons, each requiring different tool extensions. *Missing algorithmic primitives*: speculative decoding (I5.1) and prefix caching (I5.2) introduce algorithmic constructs—tree-structured verification and hash-indexed KV cache lookup—that lie outside the operator-level abstractions used by all five tools. Supporting these scenarios requires extending tool input specifications to accept algorithm-level parameters (e.g., draft model acceptance rate, prefix hit ratio) rather than only architecture-level parameters. *Missing hardware models*: FP8 training (T4.1) and INT4 inference (I5.3) require quantized arithmetic intensity models that

account for reduced-precision tensor core throughput, dequantization overhead, and mixed-precision accumulation—none of which are modeled by NeuSight’s fp16/fp32 tile decomposition or ASTRA-sim’s communication-only simulation. *Missing system-level interactions*: disaggregated serving (I5.4) and multi-model co-location (I4.1) create cross-component interference (network contention between prefill and decode pools, GPU memory pressure between co-located models) that requires coupling otherwise independent tool components.

Coverage concentration. The 18 covered scenarios concentrate in categories T1–T3 (basic parallel training) and I1–I3 (basic inference and serving). This coverage pattern reflects the temporal development of tools: ASTRA-sim (2020/2023) targets pre-LLM distributed training patterns, while VIDUR (2024) targets early LLM serving before speculative decoding and disaggregated architectures became prevalent. The field’s tool development lags deployment practice by 1–2 years. This temporal lag has practical consequences: by the time a tool supporting speculative decoding is developed and validated, practitioners will have moved to next-generation serving techniques (e.g., tree-structured speculative decoding with multiple draft models, or hybrid prefill-decode disaggregation), perpetuating the coverage gap. Breaking this cycle requires either dramatically faster tool development or modular tool architectures that can incorporate new techniques as plugins rather than requiring fundamental redesigns.

Aggregate coverage by tool. Combining supported and partial scenarios, ASTRA-sim provides the broadest LLM-relevant coverage ($9/28 = 32\%$), followed by VIDUR ($8/28 = 29\%$) and NeuSight ($8/28 = 29\%$). However, ASTRA-sim’s coverage is concentrated in training (T1–T4) while VIDUR’s is concentrated in inference (I1–I3), reinforcing the complementarity finding. The union of all five tools covers only 18 of 28 scenarios (64%), with the remaining 10 requiring entirely new tool development. Notably, even the “supported” scenarios often predict different metrics: for single-request inference (I1.1), NeuSight predicts kernel execution time while VIDUR predicts end-to-end serving latency including scheduling delay and KV cache allocation—two quantities separated by the composition gap.

Coverage quality varies within “supported” scenarios. Even among the 18 covered scenarios, support quality is uneven. For T1.1 (data-parallel GPT-2 on $8 \times A100$), NeuSight provides only per-GPU kernel time (partial) while ASTRA-sim provides full communication modeling (supported)—but neither tool produces the end-to-end iteration time that practitioners optimize. For I2.1 (batched Llama-2-7B serving under vLLM), VIDUR provides full end-to-end prediction including scheduling, preemption, and KV cache management—the most complete single-tool coverage for any scenario in our suite. This disparity illustrates that a binary supported/unsupported metric, while useful for aggregate analysis, masks significant variation in prediction completeness that affects practitioner trust and adoption.

7.7 Cross-Cutting Findings

Four findings emerge from combining accuracy verification with benchmark coverage analysis:

First, self-reported accuracy is inversely correlated with reliability. By claimed accuracy: nn-Meter (<1%) > NeuSight (2.3%) > VIDUR (<5%) > Timeloop (5–10%) > ASTRA-sim (5–15%). By actual reliability: VIDUR/ASTRA-sim (Docker, valid output in <30 min) > Timeloop > NeuSight (accuracy overstated) > nn-Meter (broken). The tools claiming the lowest error are the least reliable.

Second, the five tools are complementary, not competing. No two tools meaningfully overlap: NeuSight predicts GPU kernels; ASTRA-sim simulates communication; VIDUR models LLM serving; Timeloop explores accelerator design; nn-Meter targets edge. The field needs a *unified pipeline* combining tool strengths (Section 8).

Third, the composition gap dominates end-to-end error. NeuSight’s kernel-level 5–9% MAPE grows to 10–28% at model level. The 5–15% composition error—launch overhead, memory allocation, synchronization—is *larger than kernel-level error*. Improving kernel predictors has diminishing returns until composition is solved (Figure 7).

Fourth, 50% of modern LLM workloads lack any modeling tool. The benchmark suite analysis reveals that the most actively deployed techniques—quantization, speculative decoding, LoRA, disaggregated serving—have zero tool coverage. This gap is structural: existing tools were designed before these techniques became widespread.

Fifth, deployment robustness varies inversely with model complexity. Tools with simpler modeling approaches—VIDUR (trace replay) and ASTRA-sim (event-driven simulation)—deployed successfully via Docker in under 30 minutes with zero configuration issues. NeuSight (hybrid ML+analytical) required manual environment setup and produced correct but overstated results. nn-Meter (pure ML-augmented) failed entirely. Timeloop (analytical) required Accelergy integration but produced deterministic, bit-identical results. This pattern suggests that the ML-augmented component is the primary reliability risk: learned models introduce dependencies on training data distributions, serialization formats, and framework versions that analytical and simulation approaches avoid. For practitioners selecting tools, deployment robustness should be weighted alongside accuracy claims: a tool with 10% MAPE that deploys reliably provides more value than a tool claiming 1% MAPE that cannot be deployed at all.

Sixth, inference and training accuracy diverge systematically. Across NeuSight’s 146 configurations, inference accuracy (mean MAPE: 5.87–27.10% depending on device) is consistently better than training accuracy for NVIDIA GPUs (V100: 5.87% inf vs. 8.91% train; A100-80G: 8.63% inf vs. 7.59% train is the only exception). For AMD GPUs, the gap is larger: MI100 shows 10.80% inference vs. 15.62% training; MI210 shows 8.40% vs. 15.73%. Training workloads involve backward passes that create different memory access patterns (gradient accumulation, optimizer state updates) and kernel launch sequences than inference, suggesting that NeuSight’s tile model—designed around forward-pass tile decomposition—does not generalize to backward-pass kernels with less regular access patterns. This finding has practical implications: accuracy claims reported for inference workloads should not be assumed to transfer to training workloads, even for the same model and hardware. The divergence is particularly stark for AMD GPUs, where the ROCm software stack’s backward-pass kernel implementations differ more substantially from CUDA’s than the forward-pass implementations,

Table 10: Deployment experience for each evaluated tool.
Time excludes download. Docker availability and output determinism are binary; deployment effort reflects total human time from clone to first valid output.

| Tool | Docker | Time | Determ. | Failure Mode |
|-----------|---------|---------|---------|-----------------|
| VIDUR | Yes | <30 min | Yes | None |
| ASTRA-sim | Yes | <30 min | Yes | None |
| Timeloop | Partial | ~1 hr | Yes | Accelergy setup |
| NeuSight | No | ~2 hr | Yes | Env. config |
| nn-Meter | No | 4+ hr | N/A | Serialization |

introducing additional sources of prediction error that NeuSight’s NVIDIA-trained tile model cannot account for.

Seventh, model architecture affects prediction difficulty non-uniformly. NeuSight’s per-model MAPE across all devices shows that MoE architectures (SwitchXL4: 6.33–17.65% APE range across configurations) exhibit higher variance than dense models (OPT-13B: 0.38–10.53%; GPT-3.2.7B: 0.43–7.73%). The higher variance for MoE arises because expert routing creates workload-dependent computation patterns that a static tile decomposition cannot fully capture. This observation extends to future tools: MoE, sparse attention, and dynamic architectures will likely require workload-aware prediction mechanisms rather than architecture-only models.

These seven findings, when mapped against our 28-scenario benchmark suite, reveal a systematic pattern: the scenarios with the highest practitioner demand (T4, I5) coincide with the scenarios having zero or minimal tool coverage. Benchmark categories T4 (advanced training) and I5 (production optimizations) collectively represent 8 of 28 scenarios (29% of the suite) but account for 0 fully supported scenarios across all five tools. Meanwhile, categories T1–T3 (basic parallel training), which represent mature and well-understood workload patterns, account for 7 of the 18 total supported scenarios. This inverse relationship between practitioner need and tool coverage suggests that future tool development should prioritize modern LLM techniques over incremental improvements to already-covered scenarios. Concretely, a tool achieving even 20% MAPE on speculative decoding (I5.1) or disaggregated serving (I5.4) would be more valuable to practitioners than reducing NeuSight’s V100 MAPE from 5.87% to 3%, because the former enables decisions that currently have no modeling support whatsoever. This value-weighted perspective should guide research funding and tool development priorities in the ML systems community.

7.8 Deployment Experience and Reproducibility

Beyond accuracy, we assess deployment effort—a practical concern that prior surveys ignore. Table 10 summarizes our experience deploying each tool from scratch.

Docker availability is the strongest predictor of deployment success. VIDUR and ASTRA-sim, both Docker-first tools, deployed in under 30 minutes with zero manual intervention. Timeloop required partial manual setup for its Accelergy energy estimation plugin but produced results within one hour. NeuSight required manual Python environment configuration and model weight downloads but eventually succeeded. nn-Meter’s pip-based installation

succeeded syntactically but produced no usable output due to serialization incompatibilities. This represents the worst deployment outcome: silent success at install time masking complete failure at inference time, with no diagnostic error message until the user attempts to load a predictor—a failure pattern that undermines trust in the broader ML-augmented tool ecosystem.

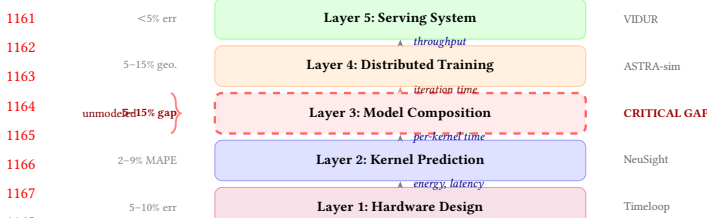
Determinism varies by methodology. All evaluated tools except nn-Meter (which produced no output) generated bit-identical results across three independent runs on the same platform. This determinism is notable for NeuSight, whose hybrid ML+analytical approach could in principle exhibit stochastic behavior; the determinism arises because NeuSight uses fixed pre-trained weights and analytical tile decomposition with no stochastic inference-time components. Deterministic outputs simplify regression testing and enable exact reproducibility—properties that should be standard but are not guaranteed by ML-augmented tools that use stochastic inference (e.g., dropout at test time, Monte Carlo sampling for uncertainty quantification).

7.9 Threats to Validity

External validity. Our venue-focused search may under-represent industry tools. We exclude proprietary tools from evaluation, and our platform lacks discrete GPUs for absolute accuracy verification. The benchmark suite’s 28 scenarios, while representative, cannot cover every production deployment pattern; emerging workloads (e.g., retrieval-augmented generation, multi-modal models) are not yet included.

Internal validity. Our evaluation covers 5 of 22 tools. Findings rest on single tool instances per methodology type—e.g., nn-Meter may be unrepresentative due to deployment failure. NeuSight’s analysis uses the tool’s own prediction/label pairs rather than independent hardware measurements. The per-device sample sizes vary (3–18 configurations), limiting statistical power for devices with few data points (e.g., P4 with only 3 configurations, A100-SXM with 3 configurations). We mitigate this by reporting both mean and worst-case APE. Our benchmark suite covers 28 scenarios, but the distribution is not uniform: training scenarios (11) outnumber inference scenarios (13), with MoE and multi-model scenarios (T4.4, I4.1) represented by only one scenario each. A more balanced suite might weight scenarios by practitioner frequency of use, but such weighting data is not publicly available. Despite these limitations, our suite provides the first standardized coverage metric for ML performance tools, enabling future evaluations to quantitatively compare tool ecosystems.

Construct validity. Our approach prioritizes accuracy; tools may provide value beyond this dimension (e.g., Timeloop’s energy breakdown for design insight, ASTRA-sim’s what-if analysis for topology exploration). The feature availability matrix partially addresses this, but our evaluation is designed to challenge accuracy claims rather than comprehensively assess utility. Additionally, our coverage criterion (supported/partial/unsupported) does not capture the quality of partial support—ASTRA-sim’s partial coverage of MoE training (T4.4), for example, provides All-to-All communication modeling but misses expert load balancing effects. A finer-grained coverage metric—e.g., percentage of scenario-relevant computations that a tool can model—would better capture partial



support quality but requires scenario-specific decomposition beyond our current scope.

Temporal validity. Our evaluation reflects tool state as of January 2026. Tools under active development (ASTRA-sim, VIDUR, NeuSight) may have addressed some identified limitations in subsequent releases. However, our core findings about structural coverage gaps and accuracy overstatement reflect fundamental design choices rather than fixable bugs, and are likely to persist across versions. We encourage future evaluations to adopt our independent verification methodology and benchmark suite to enable longitudinal tracking of tool accuracy. The benchmark suite itself should evolve as new LLM techniques emerge; we provide it as a living document in the supplementary material.

Benchmark suite validity. Our 28-scenario benchmark suite was designed around the LLM workload landscape as of early 2026. Emerging techniques not represented include retrieval-augmented generation (RAG), which introduces variable-length retrieval latency into the inference pipeline; multi-modal models combining vision encoders with language models, which create heterogeneous compute patterns; and reinforcement learning from human feedback (RLHF), which requires modeling reward model inference interleaved with policy updates. We designed the suite to be extensible: each scenario is specified by a tuple of (model architecture, hardware configuration, parallelism strategy, target metric), allowing new scenarios to be added as techniques mature without restructuring the evaluation framework. Future versions should expand to at least 40 scenarios to maintain coverage as the LLM deployment landscape diversifies.

8 Toward a Unified Simulation Pipeline

No single tool spans kernel execution through serving SLAs. Figure 6 shows five layers where 5–9% kernel MAPE grows to 10–28% at model level, driven by (i) interface heterogeneity, (ii) calibration mismatch between steady-state models and transient-dominated kernels, and (iii) feedback loops in serving schedulers.

9 Open Challenges and Future Directions

(1) Composition gap: Kernel errors of 2–3% yield 5–12% model-level error (Figure 7) with no validated pipeline. **(2) Frontier workloads:** MoE, diffusion [40], and dynamic inference lack validated tools; scaling laws [14, 22, 27, 37] predict loss but not latency (Figure 8). **(3) Hardware transfer:** Cross-family transfer (GPU→TPU→PIM [31, 46, 58]) and congestion modeling [49, 84] remain unsolved. **(4) Standardized evaluation:** No MLPerf [53, 67, 68] equivalent

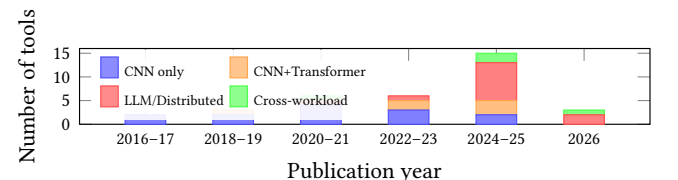
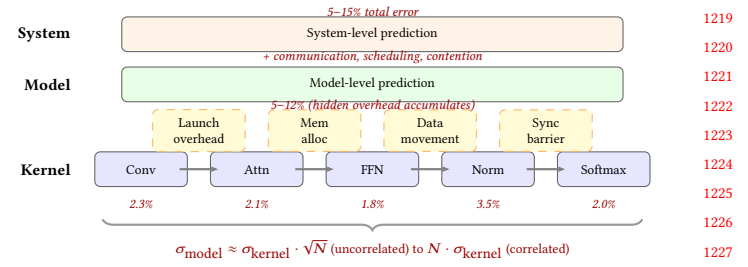


Figure 8: Workload coverage by publication period. MoE and diffusion models remain uncharacterized.

exists for simulators; portable formats [74] and continuous validation are needed. **(5) Reproducibility:** nn-Meter failed from dependency rot; containerization and CI testing are needed. **(6) Software stack evolution:** Rapidly evolving optimizations such as FlashAttention [16] invalidate performance models trained on prior kernel implementations.

10 Conclusion

We survey 22 ML performance tools and evaluate five against a 28-scenario benchmark, finding self-reported accuracy unreliable (NeuSight: 2.3% claimed vs. 5.87–27.10%; nn-Meter: no output). The 5–15% composition gap dominates total error; closing it requires validated composition models and community CI.

References

- [1] Martin Abadi, Paul Barham, Jianmin Chen, Zhifeng Chen, Andy Davis, Jeffrey Dean, Matthieu Devin, Sanjay Ghemawat, Geoffrey Irving, Michael Isard, et al. 2016. TensorFlow: A System for Large-Scale Machine Learning. In *Proceedings of the 12th USENIX Symposium on Operating Systems Design and Implementation (OSDI)*. 265–283.
- [2] Amey Agrawal, Nitin Kedia, Ashish Panwar, Jayashree Mohan, Nipun Kwatra, Bhargav S. Gulavani, Alexey Tumanov, and Ramachandran Ramachandran. 2024. Taming Throughput-Latency Tradeoff in LLM Inference with Sarathi-Serve. In *Proceedings of the 18th USENIX Symposium on Operating Systems Design and Implementation (OSDI)*. 117–134.
- [3] Amey Agrawal, Ashish Panwar, Jayashree Mohan, Nipun Kwatra, Bhargav S. Gulavani, and Ramachandran Ramachandran. 2024. VIDUR: A Large-Scale Simulation Framework for LLM Inference. In *Proceedings of Machine Learning and Systems (MLSys)*. 1–15.
- [4] Ali Bakhoda, George L. Yuan, Wilson W. L. Fung, Henry Wong, and Tor M. Aamodt. 2009. Analyzing CUDA Workloads Using a Detailed GPU Simulator. In *Proceedings of the IEEE International Symposium on Performance Analysis of Systems and Software (ISPASS)*. 163–174. <https://doi.org/10.1109/ISPASS.2009.4919648>
- [5] Abhimanyu Rajeshkumar Bambhaniya et al. 2025. HERMES: Understanding and Optimizing Multi-Stage AI Inference Pipelines. *arXiv preprint arXiv:2504.09775* (2025). Heterogeneous multi-stage LLM inference simulator with analytical modeling.
- [6] Nathan Binkert, Bradford Beckmann, Gabriel Black, Steven K. Reinhardt, Ali Saidi, Arkaprava Basu, Joel Hestness, Derek R. Hower, Tushar Krishna, Somayeh Sardashti, Rathijit Sen, Korey Sewell, Muhammad Shoaib, Nilay Vaish, Mark D. Hill, and David A. Wood. 2011. The gem5 Simulator. *ACM SIGARCH Computer Architecture News* 39, 2 (2011), 1–7. <https://doi.org/10.1145/2024716.2024718>

- [7] Shirley Browne, Jack Dongarra, Nathan Garner, George Ho, and Philip Mucci. 2000. A Portable Programming Interface for Performance Evaluation on Modern Processors. *International Journal of High Performance Computing Applications* 14, 3 (2000), 189–204. <https://doi.org/10.1177/10943420001400303> PAPI: portable API for hardware performance counters, foundational tool for performance analysis.
- [8] Kai Cai, Wei Miao, Junyu Zhu, Jiaxu Chen, Hao Shan, Huanyu Li, and Chi Zhang. 2024. Echo: Simulating Distributed Training At Scale. *arXiv preprint arXiv:2412.12487* (2024).
- [9] Tianle Cai, Yuhong Li, Zhengyang Geng, Hongwu Peng, Jason D. Lee, Deming Chen, and Tri Dao. 2024. MEDUSA: Simple LLM Inference Acceleration Framework with Multiple Decoding Heads. In *Proceedings of the 41st International Conference on Machine Learning (ICML)*. 1–15.
- [10] Zheng Cao et al. 2025. AMALI: An Analytical Model for Accurately Modeling LLM Inference on Modern GPUs. In *Proceedings of the 52nd Annual International Symposium on Computer Architecture (ISCA)*. 1–14. <https://doi.org/10.1145/3695053.3731064> Reduces GPU LLM inference MAPE from 127.56% to 23.59% vs GCo baseline.
- [11] Tianshi Chen, Zidong Du, Ninghui Sun, Jia Wang, Chengyong Wu, Yunji Chen, and Olivier Temam. 2014. DianNao: A Small-Footprint High-Throughput Accelerator for Ubiquitous Machine-Learning. In *Proceedings of the 19th International Conference on Architectural Support for Programming Languages and Operating Systems (ASPLOS)*. 269–284. <https://doi.org/10.1145/2541940.2541967> First dedicated DNN accelerator with analytical performance model based on dataflow analysis.
- [12] Tianqi Chen, Thierry Moreau, Ziheng Jiang, Lianmin Zheng, Eddie Yan, Meghan Cowan, Haichen Shen, Leyuan Wang, Yuwei Hu, Luis Ceze, Carlos Guestrin, and Arvind Krishnamurthy. 2018. TVM: An Automated End-to-End Optimizing Compiler for Deep Learning. In *Proceedings of the 13th USENIX Symposium on Operating Systems Design and Implementation (OSDI)*. 578–594.
- [13] Yu-Hsin Chen, Joel Emer, and Vivienne Sze. 2016. Eyeriss: A Spatial Architecture for Energy-Efficient Dataflow for Convolutional Neural Networks. In *Proceedings of the 43rd International Symposium on Computer Architecture (ISCA)*. 367–379. <https://doi.org/10.1109/ISCA.2016.40>
- [14] Leshem Choshen, Yang Zhang, and Jacob Andreas. 2025. A Hitchhiker’s Guide to Scaling Law Estimation. In *Proceedings of the 42nd International Conference on Machine Learning (ICML)*. 1–25. Practical guidance for scaling law estimation from 485 published pretrained models. IBM/MIT.
- [15] Weiwei Chu, Xinfeng Xie, Jiecao Yu, Jie Wang, Pavan Balaji, Ching-Hsiang Chu, Jongsoo Park, et al. 2025. Scaling Llama 3 Training with Efficient Parallelism Strategies. In *Proceedings of the 52nd Annual International Symposium on Computer Architecture (ISCA)*. 1–15. 4D parallelism for Llama 3 405B on 16K H100 GPUs. Achieves 400 TFLOPS/GPU. Meta..
- [16] Tri Dao, Dan Fu, Stefano Ermon, Atli Rudra, and Christopher Ré. 2022. FlashAttention: Fast and Memory-Efficient Exact Attention with IO-Awareness. In *Advances in Neural Information Processing Systems (NeurIPS)*, Vol. 35. 16344–16359.
- [17] Lukasz Dudziak, Thomas Chau, Mohamed S. Abdelfattah, Royson Lee, Hyeji Kim, and Nicholas D. Lane. 2024. Latency Predictors for Neural Architecture Search. In *Proceedings of Machine Learning and Systems (MLSys)*. 1–14.
- [18] Yang Feng, Zhehao Li, Jiacheng Yang, and Yunxin Liu. 2024. LitePred: Transferable and Scalable Latency Prediction for Hardware-Aware Neural Architecture Search. In *Proceedings of the 21st USENIX Symposium on Networked Systems Design and Implementation (NSDI)*. 1–18.
- [19] Paraskevas Gavriilidis et al. 2025. LIFE: Forecasting LLM Inference Performance via Hardware-Agnostic Analytical Modeling. *arXiv preprint arXiv:2508.00904* (2025). Hardware-agnostic analytical model for LLM inference performance forecasting.
- [20] Siddharth Ghosh et al. 2025. Frontier: Simulating the Next Generation of LLM Inference Systems. *arXiv preprint arXiv:2508.03148* (2025). Stage-centric simulator for MoE and disaggregated LLM inference, models expert parallelism and cross-cluster routing.
- [21] Alicia Golden et al. 2025. PRISM: Probabilistic Runtime Insights and Scalable Performance Modeling for Large-Scale Distributed Training. *arXiv preprint arXiv:2510.15596* (2025). Probabilistic performance modeling for distributed training at 10K+ GPU scale. Meta..
- [22] Alexander Hagele, Elie Bakouch, Atli Kosson, Loubna Ben Allal, Leandro Von Werra, and Martin Jaggi. 2024. Scaling Laws and Compute-Optimal Training Beyond Fixed Training Durations. In *Advances in Neural Information Processing Systems (NeurIPS)*, Vol. 37. Spotlight. Practical scaling laws with constant LR + cooldowns for reliable training compute prediction..
- [23] Ameer Haj-Ali et al. 2025. Omniwise: Predicting GPU Kernels Performance with LLMs. *arXiv preprint arXiv:2506.20886* (2025). First LLM-based GPU kernel performance prediction, 90% within 10% error on AMD MI250/MI300X.
- [24] Yanbin Hao et al. 2025. POD-Attention: Unlocking Full Prefill-Decode Overlap for Faster LLM Inference. In *Proceedings of the 30th ACM International Conference on Architectural Support for Programming Languages and Operating Systems (AS- PLOS)*. 1–15. Full overlap between prefill and decode phases for LLM inference.
- [25] John L. Hennessy and David A. Patterson. 2019. A New Golden Age for Computer Architecture. *Commun. ACM* 62, 2 (2019), 48–60. <https://doi.org/10.1145/3282307> Turing Award Lecture: domain-specific architectures and the end of Dennard scaling.
- [26] Guseul Heo, Sangyeop Lee, Jaehong Cho, Hyunmin Choi, Sanghyeon Lee, Hyungkyu Ham, Gwangsun Kim, Divya Mahajan, and Jongse Park. 2024. NeupIMs: NPU-PIM Heterogeneous Acceleration for Batched LLM Inference. In *Proceedings of the 29th ACM International Conference on Architectural Support for Programming Languages and Operating Systems (AS- PLOS)*. 1–17. NPU-PIM heterogeneous architecture for LLM inference with performance modeling. KAIST/Georg Tech..
- [27] Jordan Hoffmann, Sebastian Borgeaud, Arthur Mensch, Elena Buchatskaya, Trevor Cai, Eliza Rutherford, Diego de Las Casas, Lisa Anne Hendricks, Johannes Welbl, Aidan Clark, et al. 2022. Training Compute-Optimal Large Language Models. *arXiv preprint arXiv:2203.15556* (2022). Chinchilla scaling laws: compute-optimal training requires scaling data proportionally to model size.
- [28] Samuel Hsia, Kartik Chandra, and Kunle Olukotun. 2024. MAD Max Beyond Single-Node: Enabling Large Machine Learning Model Acceleration on Distributed Systems. In *Proceedings of the 51st Annual International Symposium on Computer Architecture (ISCA)*. 753–766. <https://doi.org/10.1109/ISCA59077.2024.00064>
- [29] Yanping Huang, Youlong Cheng, Ankur Bapna, Orhan Firat, Dehao Chen, Mia Xu Chen, Hyoukjoong Lee, Jiquan Ngiam, Quoc V. Le, Yonghui Wu, and Zhifeng Chen. 2019. GPipe: Efficient Training of Giant Neural Networks using Pipeline Parallelism. In *Advances in Neural Information Processing Systems (NeurIPS)*, Vol. 32. 103–112.
- [30] Rodrigo Huerta, Mojtaba Abaie Shoushtary, Jose-Lorenzo Cruz, and Antonio Gonzalez. 2025. Dissecting and Modeling the Architecture of Modern GPU Cores. In *Proceedings of the 58th IEEE/ACM International Symposium on Microarchitecture (MICRO)*. 369–384. Reverse-engineers modern NVIDIA GPU cores, improves Accel-Sim to 13.98% MAPE. UPC Barcelona.
- [31] Bongjoon Hyun, Taehun Kim, Dongjae Lee, and Minsoo Rhu. 2024. Pathfinding Future PIM Architectures by Demystifying a Commercial PIM Technology. In *Proceedings of the IEEE International Symposium on High Performance Computer Architecture (HPCA)*. 1–15. uPIMulator: cycle-accurate PIM simulation framework for UPMEM. KAIST..
- [32] Ryota Imai, Kentaro Harada, Ryo Sato, and Toshio Nakaike. 2024. Roofline-Driven Machine Learning for Large Language Model Performance Prediction. *NeurIPS Workshop on Machine Learning for Systems* (2024).
- [33] Anand Jayaraman, Wei-Lin Hu, Gauri Zhao, and Gennady Pekhimenko. 2023. Sia: Heterogeneity-aware, Goodput-optimized ML-Cluster Scheduling. In *Proceedings of the 29th Symposium on Operating Systems Principles (SOSP)*. 642–657. <https://doi.org/10.1145/3600006.3613175> Extends goodput optimization to heterogeneous GPU clusters for training workloads.
- [34] Norman P. Jouppi, Doe Hyun Yoon, George Kurian, Sheng Li, Nishant Patil, James Laudon, Cliff Young, and David Patterson. 2023. TPU v4: An Optically Reconfigurable Supercomputer for Machine Learning with Hardware Support for Embeddings. *Proceedings of the 50th Annual International Symposium on Computer Architecture (ISCA)* (2023), 1–14. <https://doi.org/10.1145/3579371.3589350> 4096-chip pods with 3D optical interconnect; up to 1.7x/2.1x faster than TPU v3.
- [35] Norman P. Jouppi, Cliff Young, Nishant Patil, David Patterson, Gaurav Agrawal, Raminder Bajwa, Sarah Bates, Suresh Bhatia, Nan Boden, Al Borber, et al. 2017. In-Datapath Performance Analysis of a Tensor Processing Unit. In *Proceedings of the 44th Annual International Symposium on Computer Architecture (ISCA)*. 1–12. <https://doi.org/10.1145/3079856.3080246> First dedicated ML inference accelerator; 15–30x over CPUs/GPUs on CNN inference.
- [36] Andreas Kosmas Kakolyris, Dimosthenis Masouros, Petros Vavaroutsos, Sotirios Xydis, and Dimitrios Soudris. 2025. throttLL’eM: Predictive GPU Throttling for Energy Efficient LLM Inference Serving. In *Proceedings of the IEEE International Symposium on High Performance Computer Architecture (HPCA)*. 1–14. Achieves up to 43.8% lower energy consumption for LLM inference.
- [37] Jared Kaplan, Sam McCandlish, Tom Henighan, Tom B. Brown, Benjamin Chess, Rewon Child, Scott Gray, Alec Radford, Jeffrey Wu, and Dario Amodei. 2020. Scaling Laws for Neural Language Models. *arXiv preprint arXiv:2001.08361* (2020). Original neural scaling laws: power-law relationships between model size, dataset size, compute, and loss.
- [38] Mahmoud Khairy, Zhesheng Shen, Tor M. Aamodt, and Timothy G. Rogers. 2020. Accel-Sim: An Extensible Simulation Framework for Validated GPU Modeling. In *Proceedings of the 47th International Symposium on Computer Architecture (ISCA)*. 473–486. <https://doi.org/10.1109/ISCA45697.2020.00047>
- [39] Jungho Kim et al. 2025. PyTorchSim: A Comprehensive, Fast, and Accurate NPU Simulation Framework. In *Proceedings of the 58th IEEE/ACM International Symposium on Microarchitecture (MICRO)*. 1–14. <https://doi.org/10.1145/3725843.3756045> PyTorch 2-integrated NPU simulator with custom RISC-V ISA and Tile-Level Simulation.
- [40] Jjin Kim, Byeongjun Shin, Jinha Chung, and Minsoo Rhu. 2026. The Cost of Dynamic Reasoning: Demystifying AI Agents and Test-Time Scaling from an AI Infrastructure Perspective. In *Proceedings of the IEEE International Symposium on*

1335
1336
1337
1338
1339
1340
1341
1342
1343
1344
1345
1346
1347
1348
1349
1350
1351
1352
1353
1354
1355
1356
1357
1358
1359
1360
1361
1362
1363
1364
1365
1366
1367
1368
1369
1370
1371
1372
1373
1374
1375
1376
1377
1378
1379
1380
1381
1382
1383
1384
1385
1386
1387
1388
1389
1390
1391
1392

- 1393 on High Performance Computer Architecture (HPCA). 1–14. HPCA 2026 (Jan 31–
 1394 Feb 4, 2026, Las Vegas). First comprehensive system-level analysis of AI agents;
 1395 quantifies resource usage, latency, and datacenter power consumption.
 [41] Yoongu Kim, Weikun Yang, and Onur Mutlu. 2016. Ramulator: A Fast and
 1396 Extensible DRAM Simulator. *IEEE Computer Architecture Letters* 15, 1 (2016), 45–
 1397 49. <https://doi.org/10.1109/LCA.2015.2414456> Fast extensible DRAM simulator
 1398 supporting DDRX, LPDDRx, GDDRx, WIO-X, HBMx standards.
 [42] Srivatsan Krishnan, Amir Yazdanbakhsh, Shvetank Prakash, Norman P.
 1399 Jouppi, Jignesh Parmar, Hyoukjun Kim, James Laudon, and Chandrakant
 1400 Narayanaswami. 2023. ArchGym: An Open-Source Gymnasium for Machine
 1401 Learning Assisted Architecture Design. In *Proceedings of the 50th International
 1402 Symposium on Computer Architecture (ISCA)*. 1–16. <https://doi.org/10.1145/3579371.3589049>
 1403 [43] Hyoukjun Kwon, Prasanth Chatarasi, Michael Sarber, Michael Pellauer, Angshuman
 1404 Parashar, and Tushar Krishna. 2019. MAESTRO: A Data-Centric Approach
 1405 to Understand Reuse, Performance, and Hardware Cost of DNN Mappings. In
 1406 *Proceedings of the 52nd IEEE/ACM International Symposium on Microarchitecture
 1407 (MICRO)*. 1–14. <https://doi.org/10.1145/3352460.3358292>
 1408 [44] Woosuk Kwon, Zhiuhuan Li, Siyuau Zhuang, Ying Sheng, Lianmin Zheng,
 1409 Cody Hao Yu, Joseph E. Gonzalez, Haot Zhang, and Ion Stoica. 2023. Efficient
 1410 Memory Management for Large Language Model Serving with PagedAttention.
 1411 In *Proceedings of the 29th Symposium on Operating Systems Principles (SOSP)*.
 1412 611–626. <https://doi.org/10.1145/3600006.3613165>
 1413 [45] Chris Lattner, Mehdi Amini, Uday Bondhugula, Albert Cohen, Andy Davis,
 1414 Jacques Pienaar, River Riddle, Tatiana Shpeisman, Nicolas Vasilache, and Oleksandr
 1415 Zinenko. 2021. MLIR: Scaling Compiler Infrastructure for Domain Specific
 1416 Computation. In *Proceedings of the IEEE/ACM International Symposium on Code
 1417 Generation and Optimization (CGO)*. 2–14. <https://doi.org/10.1109/CGO51591.2021.9370308> Multi-level IR infrastructure enabling cost model composition
 1418 across abstraction levels.
 1419 [46] Hyojung Lee, Daehyeon Baek, Jimyoung Son, Jieun Choi, Kihyo Moon, and
 1420 Minsung Jang. 2025. PAISE: PIM-Accelerated Inference Scheduling Engine for
 1421 Transformer-based LLM. In *Proceedings of the IEEE International Symposium on High
 1422 Performance Computer Architecture (HPCA)*. 1–14. PIM-based LLM
 1423 inference scheduling. 48.3% speedup, 11.5% power reduction. Samsung.
 1424 [47] Hayeon Lee, Sewooong Lee, Song Chong, and Sung Ju Hwang. 2021. HELP:
 1425 Hardware-Adaptive Efficient Latency Prediction for NAS via Meta-Learning.
 1426 In *Advances in Neural Information Processing Systems (NeurIPS)*, Vol. 34. 27016–
 1427 27028.
 1428 [48] Seunghyun Lee, Amar Phanishayee, and Divya Mahajan. 2025. NeuSight: GPU
 1429 Performance Forecasting via Tile-Based Execution Analysis. In *Proceedings of
 1430 the 30th ACM International Conference on Architectural Support for Programming
 1431 Languages and Operating Systems (ASPOLOS)*. 1–15.
 1432 [49] Jianbo Li et al. 2025. TrioSim: A Lightweight Simulator for Large-Scale DNN
 1433 Workloads on Multi-GPU Systems. In *Proceedings of the 52nd Annual International
 1434 Symposium on Computer Architecture (ISCA)*. 1–13. Multi-GPU DNN simulation
 1435 with lightweight approach for distributed training analysis.
 1436 [50] Shang Li, Zhiyuan Yang, Dhiraj Reddy, Ankur Srivastava, and Bruce Jacob. 2020.
 1437 DRAMsim3: A Cycle-Accurate, Thermal-Capable DRAM Simulator. *IEEE Computer
 1438 Architecture Letters* 19, 2 (2020), 106–109. <https://doi.org/10.1109/LCA.2020.2973991> Modernized DRAM simulator with thermal modeling and HMC
 1439 support.
 1440 [51] Wenxuan Liang et al. 2025. Lumos: Efficient Performance Modeling and Estimation
 1441 for Large-scale LLM Training. In *Proceedings of Machine Learning and Systems
 1442 (MLSys)*. 1–16. Trace-driven performance modeling achieving 3.3% error
 1443 on H100 GPUs for LLM training.
 1444 [52] Haocong Luo, Yahya Can Turgrul, F. Nisa Bostancı, Ataberk Olgun, A. Giray
 1445 Yaglikcı, and Onur Mutlu. 2023. Ramulator 2.0: A Modern, Modular, and Extensible
 1446 DRAM Simulator. *IEEE Computer Architecture Letters* 22, 2 (2023), 129–132.
 1447 <https://doi.org/10.1109/LCA.2023.3333759> Modular DRAM simulator with DDR5,
 1448 LPDDR5, HBM3, GDDR6 support and RowHammer mitigation modeling.
 1449 [53] Peter Mattson, Christine Cheng, Cody Coleman, Greg Diamos, Paulius Mickevicius,
 1450 David Patterson, Hanlin Tang, Gu-Yeon Wei, Peter Bailis, Victor Bittorf, et al. 2020.
 1451 MLPerf Training Benchmark. In *Proceedings of Machine Learning and Systems
 1452 (MLSys)*. 336–349. Standard ML training benchmark suite covering image classification,
 1453 object detection, NLP, recommendation, reinforcement learning.
 1454 [54] Azaz-Ur-Rehman Nasir, Samroz Ahmad Shoaib, Muhammad Abdullah Hanif, and
 1455 Muhammad Shafique. 2025. ESM: A Framework for Building Effective Surrogate
 1456 Models for Hardware-Aware Neural Architecture Search. In *Proceedings of the
 1457 62nd ACM/IEEE Design Automation Conference (DAC)*. 1–6. 97.6% accuracy
 1458 surrogate model framework for HW-aware NAS.
 1459 [55] Amir Nasr-Esfahany et al. 2025. Concorde: Fast and Accurate CPU Performance
 1460 Modeling with Compositional Analytical-ML Fusion. In *Proceedings of the 52nd
 1461 Annual International Symposium on Computer Architecture (ISCA)*. 1–15. Hybrid
 1462 analytical-ML approach achieving 2% CPI error at 5 orders of magnitude faster
 1463 than gem5.
 1464 [56] NVIDIA Corporation. 2019. Nsight Compute: Interactive Kernel Profiler. <https://developer.nvidia.com/nsight-compute>. Industry-standard GPU kernel profiling
 1465 tool with roofline analysis.
 1466 [57] Angshuman Parashar, Priyanka Raina, Yakun Sophia Shao, Yu-Hsin Chen,
 1467 Victor A. Ying, Anurag Muber, Rangharajan Venkatesan, Brucek Khailany,
 1468 Stephen W. Keckler, and Joel Emer. 2019. Timeloop: A Systematic Approach
 1469 to DNN Accelerator Evaluation. In *Proceedings of the IEEE International Symposium
 1470 on Performance Analysis of Systems and Software (ISPASS)*. 304–315.
 1471 <https://doi.org/10.1109/ISPASS.2019.00042>
 1472 [58] Jaehyun Park, Jaewan Choi, Kwanhee Kyung, Michael Jaemin Kim, Yongsuk
 1473 Kwon, Nam Sung Kim, and Jung Ho Ahn. 2024. AttAcc! Unleashing the Power of
 1474 PIM for Batched Transformer-based Generative Model Inference. In *Proceedings of
 1475 the 29th ACM International Conference on Architectural Support for Programming
 1476 Languages and Operating Systems (ASPLOS)*. 1–16. PIM-based accelerator for
 1477 batched transformer attention. Seoul National University/UICU..
 1478 [59] Adam Paszke, Sam Gross, Francisco Massa, Adam Lerer, James Bradbury, Gregory
 1479 Chanan, Trevor Killeen, Zeming Lin, Natalia Gimelshein, Luca Antiga, et al. 2019.
 1480 PyTorch: An Imperative Style, High-Performance Deep Learning Library. In
 1481 *Advances in Neural Information Processing Systems (NeurIPS)*, Vol. 32. 8024–8035.
 1482 [60] Pratyush Patel, Esha Choukse, Chaojie Zhang, Aakanksha Shah, Íñigo Goiri,
 1483 Saeed Maleki, and Ricardo Bianchini. 2024. Splitwise: Efficient Generative LLM
 1484 Inference Using Phase Splitting. In *Proceedings of the 51st Annual International
 1485 Symposium on Computer Architecture (ISCA)*. 118–132. <https://doi.org/10.1109/ISCA59077.2024.00019> Best Paper Award.
 1486 [61] Hang Qi, Evan R. Sparks, and Ameet Talwalkar. 2017. Paleo: A Performance
 1487 Model for Deep Neural Networks. In *Proceedings of the 5th International Conference
 1488 on Learning Representations (ICLR)*. <https://openreview.net/forum?id=SyV8J5lg>
 1489 [62] Aurick Qiao, Sang Keun Agrawal, Anand Jayaraman, Moustafa Mittal, Amar Altaf,
 1490 Michael Cho, and Gennady Pekhimenko. 2021. Pollux: Co-adaptive Cluster
 1491 Scheduling for Goodput-Optimized Deep Learning. In *Proceedings of the 15th
 1492 USENIX Symposium on Operating Systems Design and Implementation (OSDI)*.
 1493 1–18. Goodput estimation for co-optimizing resource allocation and training
 1494 hyperparameters.
 1495 [63] Jonathan Ragan-Kelley, Connally Barnes, Andrew Adams, Sylvain Paris, Frédéric
 1496 Durand, and Saman Amarasinghe. 2013. Halide: A Language and Compiler
 1497 for Optimizing Parallelism, Locality, and Recomputation in Image Processing
 1498 Pipelines. In *Proceedings of the 34th ACM SIGPLAN Conference on Programming
 1499 Language Design and Implementation (PLDI)*. 519–530. <https://doi.org/10.1145/2491956.2462176> Pioneered separation of algorithm and schedule with learned
 1500 cost models for autoscheduling.
 1501 [64] Samyam Rajbhandari, Jeff Rasley, Olatunji Rber, and Yuxiong He. 2020. ZERO:
 1502 Memory Optimizations Toward Training Trillion Parameter Models. In *Proceedings
 1503 of the International Conference on High Performance Computing, Networking,
 1504 Storage and Analysis (SC)*. 1–16. <https://doi.org/10.1109/SC41405.2020.00024> DeepSpeed ZeRO optimizer partitioning for memory-efficient distributed training.
 1505 [65] Mehdi Rakhshanfar and Aliakbar Zarandi. 2021. A Survey on Machine Learning-
 1506 based Design Space Exploration for Processor Architectures. *Journal of Systems
 1507 Architecture* 121 (2021), 102339. <https://doi.org/10.1016/j.sysarc.2021.102339>
 1508 [66] Saeed Rashidi, Srinivas Srinivasan, Kazem Hamedani, and Tushar Krishna. 2020.
 1509 ASTRA-SIM: Enabling SW/HW Co-Design Exploration for Distributed
 1510 DL Training Platforms. In *Proceedings of the IEEE International Symposium
 1511 on Performance Analysis of Systems and Software (ISPASS)*. 81–92. <https://doi.org/10.1109/ISPASS48437.2020.00018>
 1512 [67] Vijay Janapa Reddi et al. 2025. MLPerf Power: Benchmarking the Energy Efficiency
 1513 of Machine Learning Inference. In *Proceedings of the IEEE International Symposium
 1514 on High Performance Computer Architecture (HPCA)*. 1–14. Energy
 1515 efficiency benchmarking for ML inference workloads.
 1516 [68] Vijay Janapa Reddi, Christine Cheng, David Kanter, Peter Mattson, Guenther
 1517 Schmuelling, Carole-Jean Wu, Brian Anderson, Maxim Breshekov, Mark Duber,
 1518 et al. 2020. MLPerf Inference Benchmark. In *Proceedings of the 47th International
 1519 Symposium on Computer Architecture (ISCA)*. 446–459. <https://doi.org/10.1109/ISCA45697.2020.00045> Standard ML inference benchmark suite with server and
 1520 offline scenarios.
 1521 [69] George F. Riley and Thomas R. Henderson. 2010. The ns-3 Network Simulator.
 1522 *Modeling and Tools for Network Simulation* (2010), 15–34. https://doi.org/10.1007/978-3-642-12331-3_2
 1523 [70] Arun F. Rodrigues, K. Scott Hemmert, Brian W. Barrett, Chad Kersey, Ron Oldfield,
 1524 Marlo Weston, R. Risen, Jeanine Cook, Paul Rosenfeld, Elliott Cooper-Balis, and
 1525 Bruce Jacob. 2012. The Structural Simulation Toolkit. In *ACM SIGMETRICS
 1526 Performance Evaluation Review*, Vol. 38. 37–42. <https://doi.org/10.1145/1964218.1964225> Modular framework for system-level simulation, widely used for HPC
 1527 and interconnect modeling.
 1528 [71] Ananda Samajdar, Yuhao Zhu, Paul Whatmough, Matthew Mattina, and Tushar
 1529 Krishna. 2019. A Systematic Methodology for Characterizing Scalability of
 1530 DNN Accelerators using SCALE-Sim. In *Proceedings of the IEEE International
 1531 Conference on High Performance Computer Architecture (HPCA)*. 1–14.

- 1509 *Symposium on Performance Analysis of Systems and Software (ISPASS)*. 58–68.
 1510 <https://doi.org/10.1109/ISPASS.2019.00016> Cycle-accurate systolic array simulator for DNN accelerator DSE.
- 1511 [72] Zhuomin Shen, Jaeho Kim, et al. 2025. AQUA: Network-Accelerated Memory Offloading for LLMs in Scale-Up GPU Domains. In *Proceedings of the 30th ACM International Conference on Architectural Support for Programming Languages and Operating Systems (ASPLOS)*. 1–16. <https://doi.org/10.1145/3676641.3715983>
- 1512 Improves LLM inference responsiveness by 20x through network-accelerated memory offloading.
- 1513 [73] Mohammad Shoeybi, Mostafa Patwary, Raul Puri, Patrick LeGresley, Jared Casper, and Bryan Catanzaro. 2020. Megatron-LM: Training Multi-Billion Parameter Language Models Using Model Parallelism. In *arXiv preprint arXiv:1909.08053*.
- 1514 Intra-layer tensor parallelism for large language model training.
- 1515 [74] Srinivas Sridharan, Taekyung Heo, Jinwoo Choi, Garyfallia Yu, Saeed Rashidi, William Won, Zhaodong Meng, and Tushar Krishna. 2023. Chakra: Advancing Performance Benchmarking and Co-design using Standardized Execution Traces. *arXiv preprint arXiv:2305.14516* (2023).
- 1516 [75] Foteini Strati, Zhendong Zhang, George Manos, Ixeia Sanchez Periz, Qinghao Hu, Tiancheng Chen, Berk Buzu, Song Han, Pamela Delgado, and Ana Klimovic. 2025. Sailor: Automating Distributed Training over Dynamic, Heterogeneous, and Geo-distributed Clusters. In *Proceedings of the 30th ACM Symposium on Operating Systems Principles (SOSP)*. 1–18. Automated distributed training with runtime/memory simulation over heterogeneous resources. ETH Zurich/MIT.
- 1517 [76] Ondrej Sykora, Alexis Rucker, Charith Mendis, Rajkishore Barik, Phitchaya Mangpo Phothilimthana, and Saman Amarasinghe. 2022. GRANITE: A Graph Neural Network Model for Basic Block Throughput Estimation. In *Proceedings of the IEEE International Symposium on Workload Characterization (IISWC)*. 1–13. <https://doi.org/10.1109/IISWC55918.2022.00014>
- 1518 [77] Vivienne Sze, Yu-Hsin Chen, Tien-Ju Yang, and Joel S. Emer. 2017. Efficient Processing of Deep Neural Networks: A Tutorial and Survey. In *Proceedings of the IEEE*, Vol. 105. 2295–2329. <https://doi.org/10.1109/JPROC.2017.2761740>
- 1519 Canonical DNN accelerator taxonomy covering dataflows, data reuse, and energy efficiency.
- 1520 [78] Philippe Tillet, H. T. Kung, and David Cox. 2019. Triton: An Intermediate Language and Compiler for Tiled Neural Network Computations. In *Proceedings of the 3rd ACM SIGPLAN International Workshop on Machine Learning and Programming Languages (MAPL)*. 10–19. <https://doi.org/10.1145/3315508.3329973>
- 1521 Tile-based GPU programming with heuristic performance model for kernel generation.
- 1522 [79] Jan Treibig, Georg Hager, and Gerhard Wellein. 2010. LIKWID: A Lightweight Performance-Oriented Tool Suite for x86 Multicore Environments. In *Proceedings of the 39th International Conference on Parallel Processing Workshops (ICPPW)*. 207–216. <https://doi.org/10.1109/ICPPW.2010.38> Lightweight tools for thread/cache topology, affinity, and performance counter measurement.
- 1523 [80] Adrian Tschandl, Mohamed Awad, et al. 2025. SwizzlePerf: Hardware-Aware LLMs for GPU Kernel Performance Optimization. *arXiv preprint arXiv:2508.20258* (2025). LLM-based spatial optimization for GPU kernels, up to 2.06x speedup via swizzling.
- 1524 [81] Xizheng Wang, Qingxu Li, Yichi Xu, Gang Lu, Heyang Zhou, Sen Zhang, Yikai Zhu, Yang Liu, Pengcheng Zhang, Kun Qian, et al. 2025. SimAI: Unifying Architecture Design and Performance Tuning for Large-Scale LLM Training with Scalability and Precision. In *Proceedings of the 22nd USENIX Symposium on Networked Systems Design and Implementation (NSDI)*. 1–18. Full-stack LLM training simulator achieving 98.1% alignment with real-world results. Alibaba Cloud/Tsinghua..
- 1525 [82] Zixian Wang et al. 2025. SynPerf: Synthesizing High-Performance GPU Kernels via Pipeline Decomposition. *arXiv preprint* (2025). Under review.
- 1526 [83] Samuel Williams, Andrew Waterman, and David Patterson. 2009. Roofline: An Insightful Visual Performance Model for Multicore Architectures. *Commun. ACM* 52, 4 (2009), 65–76. <https://doi.org/10.1145/1498765.1498785>
- 1527 [84] William Won, Taekyung Heo, Saeed Rashidi, Saeed Talati, Srinivas Srinivasan, and Tushar Krishna. 2023. ASTRA-sim2.0: Modeling Hierarchical Networks and Disaggregated Systems for Large-Model Training at Scale. In *Proceedings of the IEEE International Symposium on Performance Analysis of Systems and Software (ISPASS)*. 283–294. <https://doi.org/10.1109/ISPASS57527.2023.00035>
- 1528 [85] Yannan Nellin Wu, Joel Emer, and Vivienne Sze. 2022. Sparseloop: An Analytical Approach to Sparse Tensor Accelerator Modeling. In *Proceedings of the 55th IEEE/ACM International Symposium on Microarchitecture (MICRO)*. 1–15. <https://doi.org/10.1109/MICRO56248.2022.00078>
- 1529 [86] Gyeong-In Yu, Joo Seong Jeong, Geon-Woo Kim, Soojeong Kim, and Byung-Gon Chun. 2022. ORCA: A Distributed Serving System for Transformer-Based Generative Models. In *Proceedings of the 16th USENIX Symposium on Operating Systems Design and Implementation (OSDI)*. 521–538.
- 1530 [87] Geoffrey X. Yu, Yubo Gao, Pavel Golber, and Asaf Cidon. 2021. Habitat: A Runtime-Based Computational Performance Predictor for Deep Neural Network Training. In *Proceedings of the USENIX Annual Technical Conference (ATC)*. 503–521.
- 1531 [88] Yi Zhai, Yu Cheng Wang, Peng Jiang, and Congming Kang. 2023. TLP: A Deep Learning-based Cost Model for Tensor Program Tuning. In *Proceedings of the 28th ACM International Conference on Architectural Support for Programming Languages and Operating Systems (ASPLOS)*. 833–845. <https://doi.org/10.1145/3575693.3575736>
- 1532 [89] Li Lyra Zhang, Shihao Han, Jianyu Wei, Ningxin Zheng, Ting Cao, Yuqing Yang, and Yunxin Liu. 2021. nn-Meter: Towards Accurate Latency Prediction of Deep-Learning Model Inference on Diverse Edge Devices. In *Proceedings of the 19th Annual International Conference on Mobile Systems, Applications, and Services (MobiSys)*. 81–93. <https://doi.org/10.1145/3458864.3467882> Best Paper Award.
- 1533 [90] Lianmin Zheng, Chengfan Jia, Minmin Sun, Zhao Wu, Cody Hao Yu, Amer Haj-Ali, Yida Wang, Jun Yang, Danyang Zhuo, Koushik Sen, Joseph E. Gonzalez, and Ion Stoica. 2020. Ansor: Generating High-Performance Tensor Programs for Deep Learning. In *Proceedings of the 14th USENIX Symposium on Operating Systems Design and Implementation (OSDI)*. 863–879.
- 1534 [91] Lianmin Zheng, Ruochen Liu, Junru Shao, Tianqi Chen, Joseph E. Gonzalez, Ion Stoica, and Zhihao Zhang. 2021. TenSet: A Large-scale Program Performance Dataset for Learned Tensor Compilers. In *Advances in Neural Information Processing Systems (NeurIPS)*, Vol. 34. 29876–29888.
- 1535 [92] Yinmin Zhong, Shengyu Liu, Junda Chen, Jianyu Hu, Yibo Zhu, Xuanzhe Liu, Xin Jin, and Hao Zhang. 2024. DistServe: Disaggregating Prefill and Decoding for Goodput-optimized Large Language Model Serving. In *Proceedings of the 18th USENIX Symposium on Operating Systems Design and Implementation (OSDI)*. 1–18.

1567
 1568
 1569
 1570
 1571
 1572
 1573
 1574
 1575
 1576
 1577
 1578
 1579
 1580
 1581
 1582
 1583
 1584
 1585
 1586
 1587
 1588
 1589
 1590
 1591
 1592
 1593
 1594
 1595
 1596
 1597
 1598
 1599
 1600
 1601
 1602
 1603
 1604
 1605
 1606
 1607
 1608
 1609
 1610
 1611
 1612
 1613
 1614
 1615
 1616
 1617
 1618
 1619
 1620
 1621
 1622
 1623
 1624